# ABSTRACT

Title of dissertation: FUNCTIONAL ORGANIZATION OF SOCIAL-MOTIVATIONAL BRAIN SYSTEMS DURING SOCIAL INTERACTION IN AUTISM SPECTRUM DISORDER

Dustin Moraczewski
Doctor of Philosophy, 2019

Dissertation directed by: Dr. Elizabeth Redcay
Department of Psychology

The motivation to interact with others and the feeling of reward following a social interaction is integral to the development and maintenance of successful social relationships. For those with autism spectrum disorder (ASD) successful social interaction is often more challenging relative to those who are neurotypical (NT) and atypical social reward processing may contribute to such deficits. However, our understanding of the relationship between brain systems associated with reward and higher-order social-cognitive processing during both typical and atypical development is limited. Middle childhood is an important time to examine the development of the functional relationship between these brain systems as this is a time when children's social worlds expand in size and complexity and those with ASD often fall behind. The goal of the current dissertation is to characterize the development of the functional relationship between the ventral striatum (VS)—a hub of reward processing—and other brain regions implicated in reward and social-

cognitive processing during an interactive social context in middle childhood. Using novel Bayesian multilevel modeling, Aim 1 examines VS functional connectivity within the NT group while Aim 2 examines group differences between the ASD and NT groups. Finally, given that heterogeneity is ubiquitous in both NT and ASD populations, Aim 3 takes a dimensional perspective through examining VS connectivity as a function of individual differences in autistic traits and subjective reports of social reward within the entire sample. Results suggest that participant age may be particularly important for the development of the relationship between reward and social-cognitive brain systems, such that older children of both groups exhibit greater sensitivity the absence of a social reward and to the contingency of a non-social reward. This dissertation underscores the importance of examining multidimensional heterogeneity in both NT and ASD populations.

# FUNCTIONAL ORGANIZATION OF SOCIAL-MOTIVATION BRAIN SYSTEMS DURING SOCIAL INTERACTION IN AUTISM SPECTRUM DISORDER

by

Dustin Moraczewski

Dissertation submitted to the Faculty of the Graduate School of the
University of Maryland, College Park in partial fulfillment
of the requirements for the degree of
Doctor of Philosophy
2019

Advisory Committee:
Dr. Elizabeth Redcay, Chair
Dr. Michelle Girvan
Dr. Luiz Pessoa
Dr. Tracy Riggins
Dr. Matthew Roesch

Table of Contents

# List of Tables

# List of Figures

# List of Abbreviations

| | |
|---|---|
| ASD | Autism Spectrum Disorder |
| ATL | Anterior Temporal Lobe |
| CI | Confidence Interval |
| dmPFC | Dorsal Medial Prefrontal Cortex |
| gPPI | Generalized Psychophysiological Interaction |
| fMRI | Functional Magnetic Resonance Imaging |
| ROI | Region of Interest |
| RT | Reaction Time |
| SRS | Social Responsiveness Scale |
| TPJ | Temporoparietal Junction |
| vmPFC | Ventral Medial Prefrontal Cortex |
| VS | Ventral Striatum |

# Chapter 1: Introduction

The motivation to interact with others (i.e., social motivation) and the feeling of reward following a social interaction (i.e., social reward) is a pivotal experience for the development and maintenance of successful relationships. However, for those on the autism spectrum—a disorder (ASD) characterized in part by deficits in social communication (American Psychiatric Association, 2013)—successful social interaction is often more challenging relative to those who are neurotypical. One possibility is that those with ASD experience a diminished motivation to seek out others and a reduced feeling of social reward, which could have negative effects on higher-order social-cognitive processing. While the evidence for reduced social motivation and social reward in ASD is mixed (Bottini, 2018; Clements et al., 2018), there are important gaps in the literature. First, the use of standard functional magnetic resonance imaging (fMRI) activation analysis may not fully appreciate the interactions between reward and social-cognitive brain systems and second, non-interactive social stimuli and individual differences (e.g., sample age, symptom severity) may obscure results. The goal of this dissertation is to examine the functional integration between the ventral striatum—hub of reward processing—and other regions associated with reward and social-cognitive processing during an interactive social reward within children who are both neurotypical and those on the autism spectrum.

The brain's domain-general reward system is essential to the processing of social rewards. As a central hub to this system, the ventral striatum (VS) responds in coordination with both cortical (e.g., ventral medial prefrontal cortex (vmPFC) and orbitofrontal cortex (OFC)) and subcortical regions (e.g., amygdala, ventral tegmental area) (Haber & Knutson, 2010; Sesack & Grace, 2010). One theory of reward processing, the common currency theory, suggests that the brain converts potential rewards into a single currency of valuation for the purpose of comparison and choice (Levy & Glimcher, 2012). For example, the VS is thought to signal the presence of a reward in the environment regardless of modality, while the vmPFC and OFC are thought to convert the reward into a stimulus-specific subjective hedonic representation (Levy & Glimcher, 2012; Kahnt et al., 2010; Sescousse et al., 2015). While this theory provides a framework for domain-general reward processing, it is unclear whether domain-specific social reward processing falls under the purview of the aforementioned framework or whether the complexity of social stimuli necessitate the recruitment of other brain areas.

Expanding on the common currency framework, the so-called extended common currency schema suggests that brain regions associated with higher-order social processing (e.g., temporoparietal junction (TPJ), dorsal medial prefrontal cortex (dmPFC), anterior temporal lobe (ATL), and precuneus) exert influence onto value-coding regions of the reward system (e.g., VS, vmPFC), which aids in the complex representation of social rewards (e.g., self-other distinction, knowledge of a social partner's traits, representation of a social partner's mental state) (Ruff & Fehr, 2014). The extended common currency schema stands in juxtaposition to another

theory of social reward processing: social-valuation-specific schema, which posits that social and non-social rewards are processed using distinct neural populations within the reward system (Ruff & Fehr, 2014). Using multi-variate pattern analysis methods, evidence in favor of the extended common currency schema suggests that there is an overlap between the neural populations that process both social and non-social rewards in the VS (Wake & Izuma, 2017) and vmPFC (Chavez & Heatherton, 2015), which casts doubt on the distinct neural populations predicted by the social-valuation-specific schema. Further, in addition to the reward system, regions implicated in social-cognitive processing also show greater activation during social decision making (Morishima et al., 2012; Nicolle et al., 2012; van den Bos et al., 2013) and social rewards modulate functional connectivity between regions of the reward and social-cognitive systems (Hare et al., 2010; Janowski et al., 2013; Smith et al., 2014; van den Bos et al., 2013). Thus, while social rewards certainly rely on valuation-specific regions of the reward system, it is likely that they also recruit regions of the social brain more broadly. However, it is currently unknown how these two systems co-develop in children who are typically developing as well as on the autism spectrum.

Related to the extended common currency schema, the social motivation theory of autism predicts that blunted social motivation and social reward processing has a cascading effect on social-cognitive processing (Chevallier et al., 2012). In support of this theory, those on the autism spectrum show reduced social orienting (e.g., attending to faces, responding to social sounds), less seeking and liking of social interactions (e.g., spontaneous collaboration, self-reported pleasure in response

to social situations), and diminished social maintaining behaviors (e.g., normative conversational greetings and farewells, altering one's behavior to match social context). Further, regions of the reward system (e.g., VS) show reduced response to social rewards( for review of behavioral and neural evidence of the social motivation theory see Chevallier et al., 2012). However, recent criticism suggests that researchers mistakenly infer reduced social motivation and social reward by examining ambiguous behaviors through a neurotypical lens (e.g., while attending to faces may be one index of social motivation, a reduction in this behavior is not necessarily evidence for the opposite) (Jaswal & Akhtar, 2018). Recent meta-analyses of both behavioral and neural indices of the social motivation theory have found mixed results, such that those with ASD may exhibit atypical processing of both social and non-social rewards, rather than a deficit in social reward processing specifically. In addition, methodological limitations (e.g., task design) and individual differences (e.g., age, symptom severity) may further convolute the literature (Bottini, 2018; Clements et al., 2018). This past work is limited in two ways, first, previous fMRI studies in ASD only examine neural activation and not the co-activation of diverse brain systems as predicted by the extended common currency schema and second, all previous studies have examine social rewards within a non-interactive context.

Humans experience the social world through real-time social interactions, however most prior fMRI studies of social reward and social processing more broadly within both neurotypical and ASD samples use static, non-interactive social stimuli (e.g., pictures of smiling faces). An interactive context has been shown to fundamentally alter processing within domains such as language processing (Pickering &

Garrod, 2013), joint attention (Sebanz et al., 2006), and social attention (Risko et al., 2012) due to the fact that real-time social interaction engenders a reciprocal and dynamic rhythm that proves important for interpersonal understanding (Schirmer et al., 2016; Zaki & Ochsner, 2009). In addition, an interactive context has been shown to modulate brain activity in neurotypical adults within regions implicated in reward and social-cognitive processing, even in the absence of explicit reward and/or social-cognitive task demands (Redcay et al., 2010; Rice & Redcay, 2016; Schilbach et al., 2010). The recruitment of reward and social-cognitive systems during social interaction suggests that 1) aspects of social interaction may be intrinsically rewarding and 2) an interactive context may automatically activate the representation of a social partner in preparation for interaction, respectively (Redcay & Warnell, 2018).

While neuroimaging studies of real-time social interaction are becoming more prevalent in neurotypical samples, relatively fewer experiments have examined the neural bases of an interactive context in ASD, an important gap given that social deficits in ASD are often exacerbated in real-world contexts (Schilbach et al., 2013). Results from the few studies that have examined the neural bases of social interaction in ASD suggest that regions within the reward (e.g., VS) and social-cognitive (e.g., TPJ, dmPFC) systems are hypoactive in ASD relative to neurotypical controls (Assaf et al., 2013; Redcay et al., 2013). Thus, for an ecologically-valid assessment of the functional relationship between the reward and social-cognitive brain systems in both neurotypical development and ASD, researchers must examine brain function during an interactive context.

In addition to limitations in task design, another possible factor contributing

to the inconclusive meta-analyses on the social motivation theory (Bottini, 2018; Clements et al., 2018) is sample age. Clements et al., 2018 found that mixed support for atypical social reward processing in ASD could be driven by age-related differences in samples, such that younger ASD samples exhibited hypoactivation within the VS in response to social rewards but not the older samples (Clements et al., 2018). Middle childhood (between the ages of 8- and 12-years old) is an important time to examine the neural bases of social reward in ASD as those on the spectrum increase in rates of social withdraw (Anderson et al., 2011) and fall behind with respect to theory of mind abilities (Bal et al., 2013). Further, this age range is an important time for typical social and neural development. As children's social sphere's expand in both size and complexity (Carr, 2017), social competence (Monahan & Steinberg, 2011; Parker et al., 2015) and performance on laboratory-based theory of mind tasks also increase (Apperly et al., 2011; Dumontheil et al., 2010; Rice et al., 2016). Finally, middle childhood is also a time of functional specialization within the social brain for social reward (Warnell et al., 2017) and social-cognitive processing (Gweon et al., 2012; Saxe et al., 2009), as well as more general functional network organization (de Bie et al., 2012; Muetzel et al., 2016; Supekar et al., 2010). Thus, middle childhood provides an important window in which to examine the interaction between reward and social-cognitive brain systems in neurotypical and ASD samples during a real-time social interaction (Redcay & Warnell, 2018).

The current dissertation examines the functional relationship between a hub of the reward network (VS) and other regions implicated in reward and social-cognitive

processing during a real-time social interaction in children who are neurotypical and those on the autism spectrum. We use a rewarding social interaction task (Warnell et al., 2017) that can examine the motivation to initiate a social interaction through sharing self-relaant information with a social partner as well differentiate between the receipt of a social versus non-social reward, as well as reward contingency. Using a novel Bayesian multilevel modeling approach (G. Chen et al., 2019), we leverage the pooled information between multiple regions of interest within the reward and social-cognitive brain systems. In addition, to examine the specificity of our results, we also include control regions within the motor, primary auditory, and visual cortices.

In Aim 1, we focus on characterizing how VS functional connectivity is modulated by the various task conditions within the neurotypical (NT) sample (N = 63). We hypothesize that VS functional connectivity will increase in response to the motivation to interact with a social partner within both the reward and social-cognitive ROIs, but not the control regions. With respect to social reward, we also expect that VS functional connectivity will increase within the reward and social-cognitive ROIs, but not the control regions. Further, we expect that this effect will be specific to social reward and not merely the presence of a social partner (i.e., reward contingency by partner type interaction). We also expect that VS functional connectivity as described above will increase as a function of age. In Aim 2, we examine group differences between age- and sex-matched ASD and NT samples (N = 31 in each group). We expected that VS functional connectivity to all conditions will be blunted in the ASD compared to the NT sample. In addition, given that children

with ASD often fall behind socially during this age, we predict that age will not be related to increases in VS functional connectivity. Finally, given that heterogeneity is ubiquitous in both ASD and NT populations, in Aim 3 we take a dimensional approach to individual differences in the entire sample (Easson & McIntosh, 2019; Elton et al., 2016). Here we examine VS functional connectivity as a function of individual differences in participant's post-scan subjective reports of social motivation and social reward, as well as autistic traits as reported on a parent questionnaire (Constantino & Todd, 2003). We hypothesize that VS functional connectivity will be positively related to subjective reports of motivation and reward and negatively related to autistic traits. This dissertation is the first study to examine functional connectivity between regions implicated in reward and social-cognitive processing during a real-time social interaction in either NT or ASD samples and will have important implications for understanding how the typically- and atypically-developing brain processes rewarding social interactions.

# Chapter 2: Methods

## 2.1 Participants

We recruited a cross-sectional sample of children between the ages of 8 and 14. Overall 89 families with children who are neurotypical (NT sample) and 44 families with children with autism (ASD sample) participated in the study. Families in the NT sample were recruited from University of Maryland's Infant and Child Studies database, whereas families in the ASD sample were recruited through a combination of external advertisement (e.g., fliers at public schools) and relevant electronic mailing lists. Participants were native English speakers and had normal hearing and normal or corrected-to-normal vision. Further, participants in the NT sample had no first-degree relatives with autism. Autism diagnosis in the ASD sample was confirmed through the administration of the Autism Diagnostic Observation Schedule, Second Edition (ADOS-2) (Lord et al., 1989) given by a research-reliable practitioner. Participants in both samples came into the lab for a behavioral battery (see Behavioral Measures). Then, during a separate visit, participants came to the Maryland Neuroimaging Center for an MRI scan (see Interactive Chat Task). Parents were monetarily compensated and children were given a toy for their participation. All protocols were approved by the University of Maryland Institutional Review

Board and implemented in accordance with relevant guidelines and regulations.

After data collection, 38 participants were excluded from analysis for either failure to complete the scanning task (4; 2 NT, 2 ASD), failure to believe the live social interaction illusion (11; 9 NT, 2 ASD), or excessive head motion (see fMRI Preprocessing) (23; 14 NT, 9 ASD). Our final sample consisted of 63 participants in the NT group (28 female, mean age = 11.04, sd = 1.61) and 31 participants in the ASD group (3 female, mean age = 12,00, sd = 2.01). For between-group comparisons we mean-matched an NT group to match the ASD group on age-, sex-, and IQ so that both groups consisted of 31 participants (3 females in each group) and did not differ with respect to age (t(60)=0.87, p=0.39), head motion (t(60)=1.26, p=0.21), or full scale IQ (t(60)=0.43, p=0.67) (see figure 2.1 for age and IQ distributions for the matched groups).

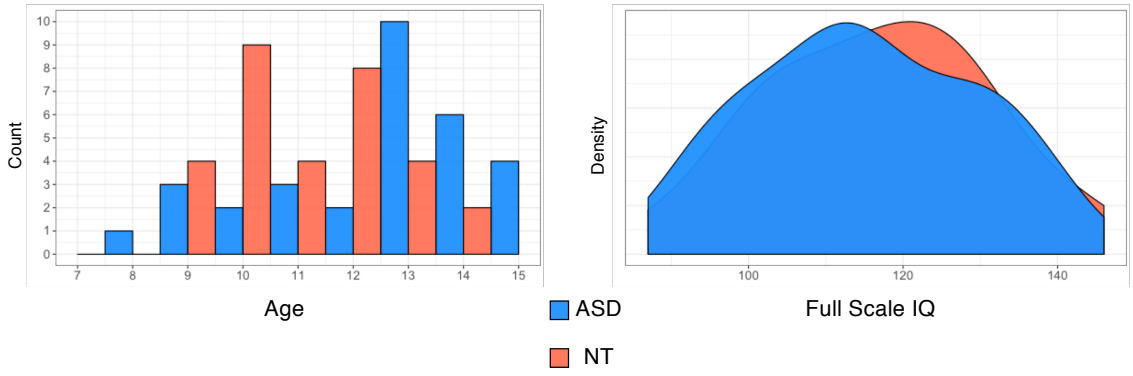


Figure 2.1: Age and full scale IQ distributions for the matched ASD and NT samples.

## 2.2 Behavioral Measures

Participants were given the Kaufman Brief Intelligence Battery, which measures both verbal and non-verbal IQ (Kaufman & Kaufman, 2004). To ensure that our results are not due to individual differences in participant intelligence, we use the composite full-scale IQ as a covariate in all of our functional connectivity analyses. In addition, parents were given the Social Responsiveness Scale (SRS) to measure autistic traits in their children along a continuum. (Bölte et al., 2008; Constantino & Todd, 2003). In the current study we use the total raw score as an index of autistic traits and the motivation domain sub-scale as an index of social motivation.

## 2.3 Interactive Chat Task

### 2.3.1 Pre-scan procedure

The procedure and task design in this dissertation are identical to the task reported in Warnell et al., 2017. Before the fMRI scan all participants underwent a mock scanner protocol to ensure that they understood the task and to establish the live social interaction illusion. First, participants were given a short practice session analogous to the MRI task in which they answered 'yes' or 'no' questions about themselves (e.g., "I like cookies"). Second, once the experimenter was confident that participants could answer the questions in the appropriate time window (3.5 seconds, based on the timing in the Task Design), the participant was removed from the mock scanner and given a full description of the interactive chat task.

For the task description, participants were told that they would answer questions about themselves and that sometimes their answers would be shared with a peer who is in another lab. The experimenter explained that sometimes the peer is be able to send responses back to the participant (i.e., "Me too!" and "That's not what I picked"). This dissertation will refer to the "Me too!" response as the peer-agree reply and "That's not what I picked" as peer-disagree reply. The experimenter also explained that sometimes the peer is not able to respond because they are sometimes required to play another game at the same time, but that the peer will still see the participant's answers. When the peer is away, participants are presented with an "I'm away" message from the peer (subsequently referred to as a peer-away reply). The experimenter then explained that sometimes the participant's answers are sent to a computer, which will randomly choose an answer that either matches ("Matched!") or does not match ("Mismatched!") the participant's answer. These reply types will be referred to as computer-agree and computer-disagree, respectively. Participants were then, told that the computer occasionally becomes disconnected and is unable to randomly choose an answer. For these responses, participants were presented with a "Disconnected" message (subsequently referred to as computer-away). Finally, following the explanation of the task, the experimenter asked a series of comprehension questions to ensure that the participants understood the difference between the peer and computer conditions, as well as the different reply types. See Figure 1 for a detailed description of the task and response types.

After the explanation of the task, participants were told that it was time to

find a chat partner in another lab, after which the experimenter took a photograph of the participant under the guise of sending it to the other participating labs. Then, participants were allowed to choose their chat partner from two images of age- and sex-matched peers (images taken from either Egger et al., 2011 or Google images). Since previous work has shown that responses from desirable peers are more salient (Guyer et al., 2009), we allowed participants to choose their chat partner to increase motivation.

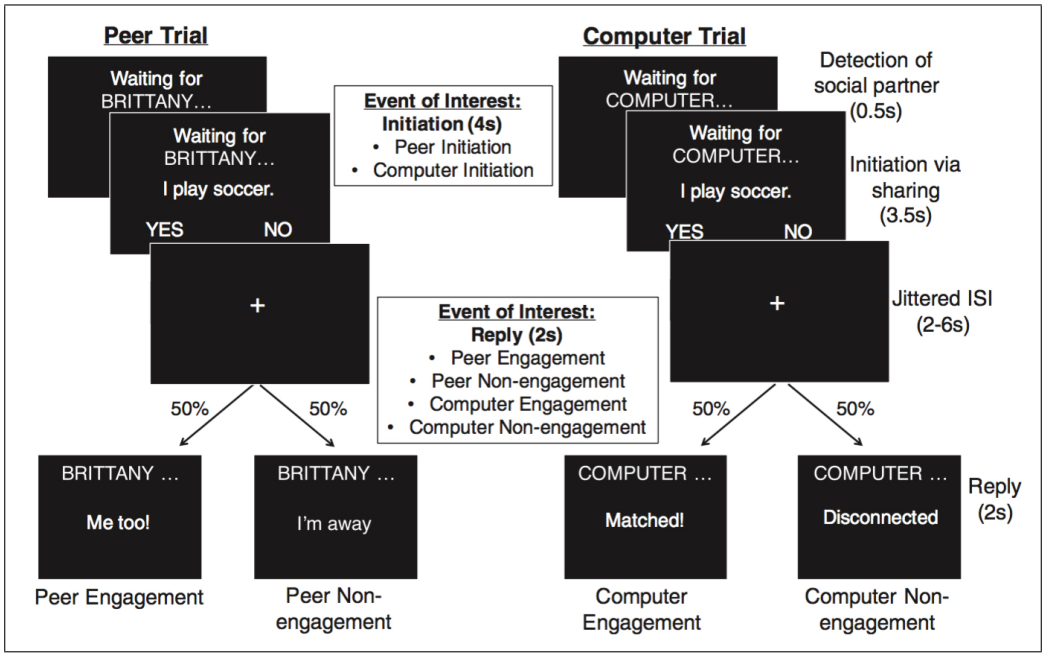


Figure 2.2: Interactive chat task design, reproduced from Warnell et al., 2017

### 2.3.2 Task Timing

For the fMRI experiment, each trial began with a 0.5 second cue where participants were informed of which chat partner they would have for the upcoming

trial (i.e., peer's name or computer). The cue was then immediately followed by a 3.5 second event where participants answered a self-relevant question (e.g., "I have a cat"). This period of initiating a social interaction (consisting of both the cue and question) for each condition will subsequently be referred to as peer-initiation and computer-initiation. The initiation period was then followed by a 2-6 second jittered (exponentially distributed around a mean of 3.5 seconds) inter-stimulus interval (ISI) in which participants viewed a fixation cross. After the ISI, participants viewed a 2 second outcome event where they receive a response from their partner (i.e., peer-agree, peer-disagree, peer-away, computer-agree, computer-disagree, computer-away). Finally, each trial was separated by another 2-6 second jittered (exponentially distributed around a mean of 3.5 seconds) inter-trial interval (ITI) fixation. Thus, due to the jittered ISI and ITI, we are able to statistically disentangle the initiation from the outcome events (Ruge et al., 2009). In addition, each run is preceded with a 15 second fixation to account for magnetization equilibration and followed by a 10 second fixation to account for hemodynamic lag. See Figure 2.2 for a detailed description of the task timing.

Participants viewed 52 trials of each initiation type (peer and computer) over 4 runs in the scanner. The self relevant questions presented during the initiation period were counterbalanced across partner and response type. For the reply period, participants received 24 trials of each of the following response types: peer-agree, peer-away, computer-agree, computer-away. While the trials were predominately agree or away, participants also received 2 disagreement trials per run to make the interaction seem more naturalistic. Importantly, the current task is designed to test

social motivation and social reward and not social rejection, negative partner evaluation, or social exclusion (Blackhart et al., 2009; Kross et al., 2011). Thus, in the interest of minimizing disagreement while maintaining ecological validity, we chose to give participants relatively few disagree trials and these trials were subsequently excluded from analyses (Warnell et al., 2017). On trials where participants failed to answer the question in the alloted time window (3.5 seconds), they received an away message. Both the disagree trials and the initiation and reponse events from trials where participants did not answer in time were modeled as events of no interest and excluded from analysis. The task is designed as a 2x2 factorial (partner - peer and computer by contingency - agree and away). For the current study, we changed stimulus presentation software after a majority of our data had been collected. Stimuli for 84 participants in the final sample were presented using the Psychophysics Toolbox (Kleiner et al., 2007) whereas stimuli for the remaining 10 participants were presented using PsychoPy (version 1.83.04) (Peirce, 2007).

### 2.3.3 Post-scan Questionnaire

Immediately following the scan, participants were given a post-scan questionnaire to measure their subjective impressions of the task. On a 5-point Likert-type scale, participants rated their motivation and subjective feeling of reward for each of the two partners (peer and computer) and response types (agree and away). Specifically, participants were asked "How much did you want to see (peer's name / the computer's) answer to your question?" as an index of their motivation. Participants

were asked how did you feel when (peer's name / the computer) agreed with you" and "How did you feel when (peer's name / the computer) was away (or disconnected) and did not respond?" to index of their feeling of reward. In addition, participants were asked to give their open-ended impressions regarding the experiment and if there was anything more to the study than they were told (in order to probe the success of the social deception).

## 2.4 Image Acquisition

MRI data were acquired using a Siemens 3 Tesla MAGNETOM Trio scanner using a 32-channel head coil. A high-resolution T1-weighted magnetization prepared rapid gradient-echo (MPRAGE) image sequence (192 contiguous sagittal slices; slice matrix = 512 x 512; voxel size = 0.90 x 0.45 x 0.45mm; TR/TW/inversion = 1900/2.32/900ms; flip angle = 9°). Four runs of functional data were acquired using an interleaved acquisition T2*-weighted echp planar image (EPI) sequence (40 interleaved axial slices; slice matrix = 64 x 64; voxel size = 3 x 3 x 3.3mm; TR/TE = 2200/24ms; flip angle = 78°). 168 EPI volumes were collected per run, however, due to a change in stimulus presentation software, we altered the timing parameters to add one a functional volume onto each run. Thus, 10 of the 94 participants in the final sample have 170 rather than 168 volumes per run, however the stimulus timing did not change. For all functional runs the first 4 volumes of EPI data were automatically discarded to allow for magnetization equilibrium.

## 2.5 fMRI Preprocessing

The functional data were preprocessed with in-house scripts using tools in the AFNI software package (version 18.0.18) (Cox, 1996). First, the functional data were corrected for offsets in interleaved slice-time acquisition. Then, transformation matrices were created to register the structural T1-weighted image and all functional volumes to a common functional base and for MNI normalization. All transformations (co-registration and normalization) were then completed during the same step to minimize interpolation of the functional data. Finally, the functional data were smoothed using a 5mm full-width half-maximum Gaussian kernel and scaled, such that each voxel had a mean of 100.

The realignment parameters created during the co-registration step were used to quantify head motion and create regressors of no interest for the functional connectivity analysis. Frame displacement was defined as $FD_i = |\Delta d_{ix}| + |\Delta d_{iy}| + |\Delta d_{iz}| + |\Delta \alpha_i| + |\Delta \beta_i| + |\Delta \gamma_i|$ (Power et al., 2012). Runs were excluded if $> 10\%$ of the volumes exceeded 1mm in translation and/or rotation or the run had a maximum frame displacement of 4mm. At this step, 14 participants in the NT group and 9 participants in the ASD group were excluded from further analysis for having fewer than 3 runs that met our criteria for head motion. Within the final sample NT sample, 19 participants contributed 3 runs in the analysis, whereas the other 44 participants contributed all 4 runs. Within the matched NT and ASD groups, both groups consisted of 9 participants in which only 3 runs were included in the analysis.

## 2.6 First-level Functional Connectivity Analysis

To examine the context-dependent functional relationship between the VS and brain regions implicated in motivational and social-cognitive processing, we utilized a generalized psychophysiological interaction (gPPI) analysis (McLaren et al., 2012). Previous simulation analysis has shown that the gPPI framework more accurately estimates task-based functional connectivity for tasks with trial numbers and event durations similar to that of the current study (Cisler et al., 2014). To define our VS seed region of interest (ROI), we constructed a 3.5mm sphere around the bilateral coordinates associated with the inferior VS, identified using resting state functional connectivity (MNI coordinates = ±9, 9, -8) (Di Martino et al., 2008) (Figure 2.3). The mean preprocessed time series within the VS ROI was first extracted from each run and then deconvolved to represent a time series within the neural domain. The stimulus timing was used to create a binary 'on' and 'off' time series for each condition of interest (peer-initiation, computer-initiation, peer-agree, peer-away, computer-agree, and computer-away). The neural time series was then multiplied by the binary time series for each condition and convolved back to the BOLD domain, resulting in six interaction terms.

Since the short temporal relationship between the initiation and reply events may induce response overlap (Ruge et al., 2009), we estimated FC in a two-step regression analysis. For the initiation phase of the task, we first regressed out the task information related to the reply events. Here, the first voxelwise regression estimated the mean response for all reply events for the factors of interest (peer-agree,

Figure 2.3: Ventral Striatum Seed Region.

peer-away, computer-agree, computer-away), as well as separate regressors for the reply events where participants did not answer in time during the corresponding initiation event and for disagree replies, respectively. The mean response for all events in all regressions were modeled using a BLOCK hemodynamic response function in AFNI. We also included de-meaned motion parameters, their derivatives, and low-frequency drift terms as nuisance regressors. In addition, we censored volumes where head motion was greater than 1mm in translation and/or rotation from the model (Power et al., 2014). We then conducted a second regression using the residuals of the first regression. The second regression estimated mean response for the initiation events of interest (peer-initiation and computer-initiation), as well as a regressor of no interest corresponding to the initiation events where participants did not answer in time. For terms relevant to functional connectivity, we included the time series from the seed VS ROI, as well as the two gPPI terms corresponding to the peer-initiation and computer-initiation events. Here the contrast of interest examines voxels that exhibit greater functional connectivity during the peer initiation compared to the computer initiation events (peer-initiation>computer-initiation).

For the reply phase of the task, we first regressed out the task information related to the initiation events. Here, the first voxelwise regression estimated the mean response for all initiation events (peer-initiation and computer-initiation), as well as separate regressors for the initiation events where participants did not answer in time. As with the previous analysis, we included the same nuisance regressors for head motion and drift. The second regression estimated mean response for all reply events of interest (peer-agree, computer-agree, peer-away, computer-away), as well as reply events where participants did not answer in time during the corresponding initiation event and disagree replies, respectively. For functional connectivity, we included the time series from the seed VS ROI, as well as the four gPPI terms corresponding to the peer-agree, computer-agree, peer-away, and computer-away conditions. Here we have three statistical tests of interest: the main effect of each factor (peer>computer and agree>away) and the interaction between partner and response type. Finally, four pairwise contrasts were created to examine the directionality of the aforementioned effects (peer-agree>computer-agree, peer-agree>peer-away, peer-away>computer-away, and computer-agree>computer-away).

## 2.7 Regions of Interest

While the aforementioned gPPI analysis was conducted at the voxel level, our hypotheses examined the relationship between the VS and multiple *a priori* ROIs. Given it's role in the conversion of a reward into a subjective hedonic value (Levy & Glimcher, 2012; Kahnt et al., 2010; Sescousse et al., 2015), we examined the vmPFC

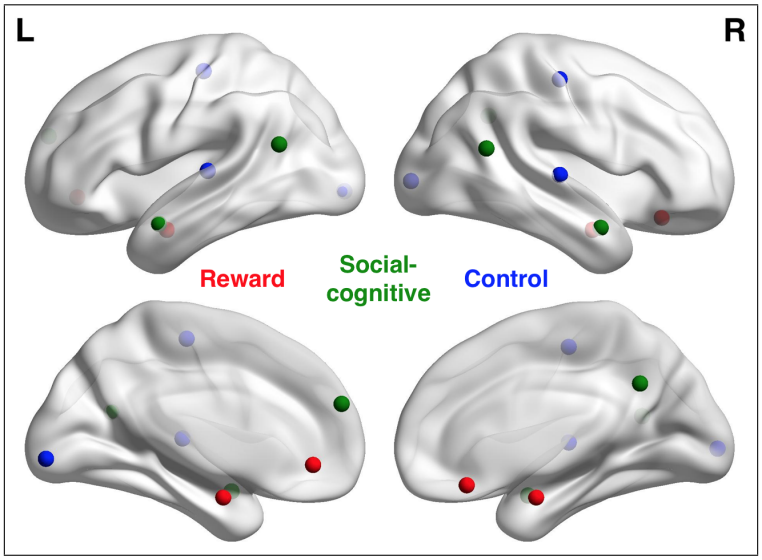


Figure 2.4: Functional Connectivity Regions of Interest.

as another node within the reward system. Here we defined bilateral vmPFC ROIs from a meta-analysis that examines brain regions implicated in the computation of subjective value (Clithero & Rangel, 2014). Due to it's role in both reward and social processing we defined bilateral amygdala ROIs from a study that examined the relationship between amygdala functional connectivity and social network size (Bickart et al., 2012). To define ROIs within the social-cognitive system (dmPFC, ATL, TPJ, and precuneus), we used coordinates from a meta-analysis of theory of mind tasks (Schurz et al., 2014). While most ROIs were defined bilaterally and then averaged, only one region was created for the the mideline ROIs (i.e., dmPFC and precuneus). We chose to keep the TPJ as separate left and right hemisphere regions because previous work suggests that there may be a differential role in social processing within the left compared to the right hemisphere TPJ (Saxe & Wexler, 2005; Schurz et al., 2013) Finally, to ensure that our observed effects are specific to

| | ROI | Left | | | Right | | |
|---|---|---|---|---|---|---|---|
| | | x | y | z | x | y | z |
| Reward | vmPFC | -2 | 40 | -6 | 4 | 30 | -16 |
| | Amygdala | -28 | -4 | -22 | 28 | -4 | -22 |
| Social-cognitive | dmPFC | -1 | 54 | 24 | - | - | - |
| | ATL | -51 | 0 | -19 | 53 | 0 | -21 |
| | TPJ | -53 | -59 | 20 | 56 | -56 | 18 |
| | Precuneus | 4 | -55 | 34 | - | - | - |
| Control | Motor | -34 | -22 | 56 | 40 | -20 | 52 |
| | Auditory | -48 | -24 | 7 | 59 | -20 | 5 |
| | Visual | -5 | -91 | -3 | 13 | -93 | 2 |

Table 2.1: Region of Interest coordinates.

our regions of interest, we used NeuroSynth (Yarkoni et al., 2011) to define control regions within the bilateral motor, auditory, and visual cortices. All ROIs were created by drawing a sphere with a 5mm radius centered on the coordinates in Table 2.1 (Figure 2.4).

## 2.8 Second-level Bayesian Multilevel Model

While first-level analysis occurred at the voxel level, for each participant we then extracted the mean $\beta$ estimate for each contrast from each of the aforementioned ROIs for the a second-level Bayesian multilevel model (BML) (G. Chen et al., 2019). This BML framework incorporates data from all ROIs for each contrast into the same model, which simultaneously leverages the shared variance between ROIs for a more accurate estimation of the effects and removes the multiple comparison issue when constructing an independent model for each ROI. For each model, we estimate the outcome $\beta$ value for each contrast from a serious of explanatory fixed and random effects. In terms of random effects, each model allows the intercept to

vary by participant and ROI, as well as allowing the slope of each fixed effect to vary for each ROI.

For Aim 1, which examines the modulation of VS functional connectivity by task event, our fixed effect of interest is the intercept, which corresponds to the average effect of each contrast value (e.g., a value greater than 0 for the peer-initiation > computer-initiation contrasts is evidence that there is greater VS functional connectivity during the peer compared to the computer initiation trials). The models in Aim 1 also control for participant age, condition-specific head motion, and full-scale IQ. In Aim 2, we examine group differences between the ASD group and an age- and sex-matched NT sample. Here our fixed effect of interest is how group membership effects the outcome contrast value, while also controlling for participant age, condition-specific head motion, and full-scale IQ. In Aim 3, we examine individual differences within the entire sample (all NT and ASD). Here our fixed effects of interest are participant age, participant reports on the post-scan questionnaire and scores on the SRS, while also controlling for group membership, participant age, condition-specific head motion, and full-scale IQ. With respect to the post-scan questionnaire, we had one relevant question for each condition of interest (i.e., peer-initiation, computer-initiation, peer-agree, peer-away, computer-agree, computer-away). Since our outcome measures for each BML are a functional connectivity contrast $\beta$ value, we converted the post-scan responses into contrast values as well. That is, for the outcome contrast of peer-initiation > computer-initiation, we subtracted the post-scan question corresponding to how much participants wanted to see the peer's response from how much participant's wanted to see the computer's response. Thus,

each functional connectivity contrast had a corresponding explanatory behavioral contrast. All quantitative variables (i.e., age, head motion, IQ, post-scan reports, and SRS) were mean-centered and the factor of group was coded as 0 for the ASD group and 1 for the NT group. The results from each model are presented as the posterior distribution surrounding each effect of interest for each ROI. If the 95% quantile interval does not include 0 then we interpret this result as reasonable evidence that the contrast $\beta$ outcome is modulated by the effect of interest.

## 2.9 Exploratory Whole Brain Analysis

We then followed up our ROI analysis with an exploratory whole brain analysis to examine whether VS functional connectivity was modulated within regions outside our *a priori* ROIs. All first-level voxelwise functional connectivity maps were entered into a second-level analysis (peer-computer initiation, main effect of partner reply, main effect of reward contingency, partner type by contingency interaction, peer agree-away, peer-computer agree, peer-computer away, and computer agree-away). We used a mixed effects multilevel analysis (3dMEMA in AFNI) which weights the $\beta$ contrast coefficients by their corresponding $t$ statistics (G. Chen et al., 2012). All second-level group functional connectivity maps were then thresholded at a voxelwise $p < 0.001$ and cluster corrected at $k$=19 (accounting for spatial autocorrelation) to ensure a FWE of $p$ <0.05.

# Chapter 3: Results

## 3.1 Aim 1: Functional Connectivity in the NT Group

### 3.1.1 Initiation Event

As reported on the post-scan questionnaire, all participants in the final sample believed that they were chatting with a peer in real-time. During the initiation event participants were given a cue that signaled which chat partner would participate in the current trial and then a subsequent self-relevant statement to answer. On the post-scan questionnaire, we used participant ratings on the questions "How much did you want to see (peer's name or the computer's) answer to your question" as an index of motivation to initiate the interaction.

Using a mixed-effects linear model to examine the effect of condition on participant reaction time (RT) we found weak evidence that participants in the NT group responded quicker during the peer compared to the computer trials ($\beta_{peer}$=-0.03, 95% CI [-0.05,0.00], $t(62)$=-2.09, $p$ <0.05) (Figure 3.1a). Further, as measured on the post-scan questionnaire, we found that participants reported greater motivation to see the peer's response compared to the computer ($\beta_{peer}$=1.29, 95%CI [0.94 1.63] $t(62)$=7.25, $p$ <0.001) (Figure 3.1b).

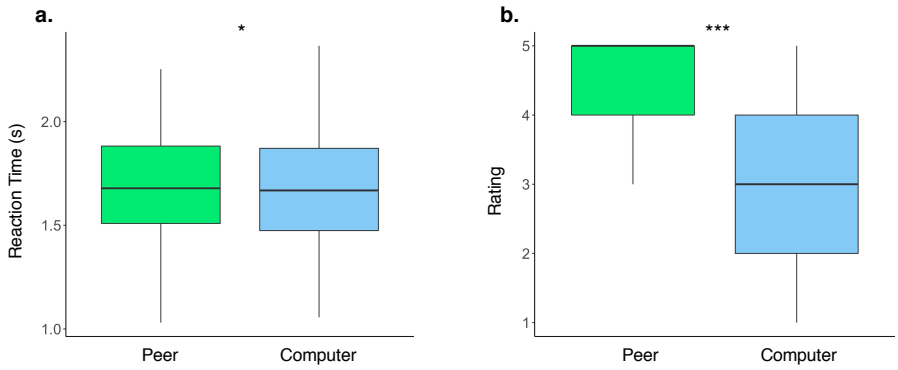


Figure 3.1: Aim 1 Initiation event behavioral results for NT group. a) Boxplot of reaction time for both the peer and computer trials. b) Boxplot of self-report post-scan questionnaire ratings of subjective motivation to see each chat partner's response. *$p$ <0.05, ***$p$ <0.001

In terms of functional connectivity between the VS and the reward (vmPFC, amygdala), social-cognitive (dmPFC, TPL, left TPJ, right TPJ, and precuneus), and control (motor, auditory, and visual) ROIs, we used a Bayesian multilevel model (G. Chen et al., 2019) which incorporated average 1st-level peer-computer initiation contrast values from all ROIs within all participants into the same model. For the current aim, our focus is on the posterior distribution of the model intercept which denotes the confidence surrounding 1st-level contrast value (peer-computer initiation, in this case). In addition, the model accounted for the nested nature of the data (contrast $\beta$ values within ROIs within participants) and controlled for fixed-effects of head motion, age, and IQ. For the ROIs within the reward and the social-cognitive systems, the 95% confidence interval (CI) posterior distributions surrounding the model intercept overlapped with 0, which suggests little evidence that the peer condition modulated VS functional connectivity more so than the computer condition during the initiation event. In addition, we did not detect an

an effect within the control ROIs. See Figure 3.2a for the posterior distributions for each ROI and Table A.1 for the mean, standard deviation, and confidence intervals surrounding the posterior distributions of the intercept. Similar to our ROI findings, exploratory VS to whole brain functional connectivity analysis did not reveal any statistically significant clusters for the peer-computer initiation contrast (voxelwise $p$ <0.001, $k$=19, FWE=$p$ <0.05).

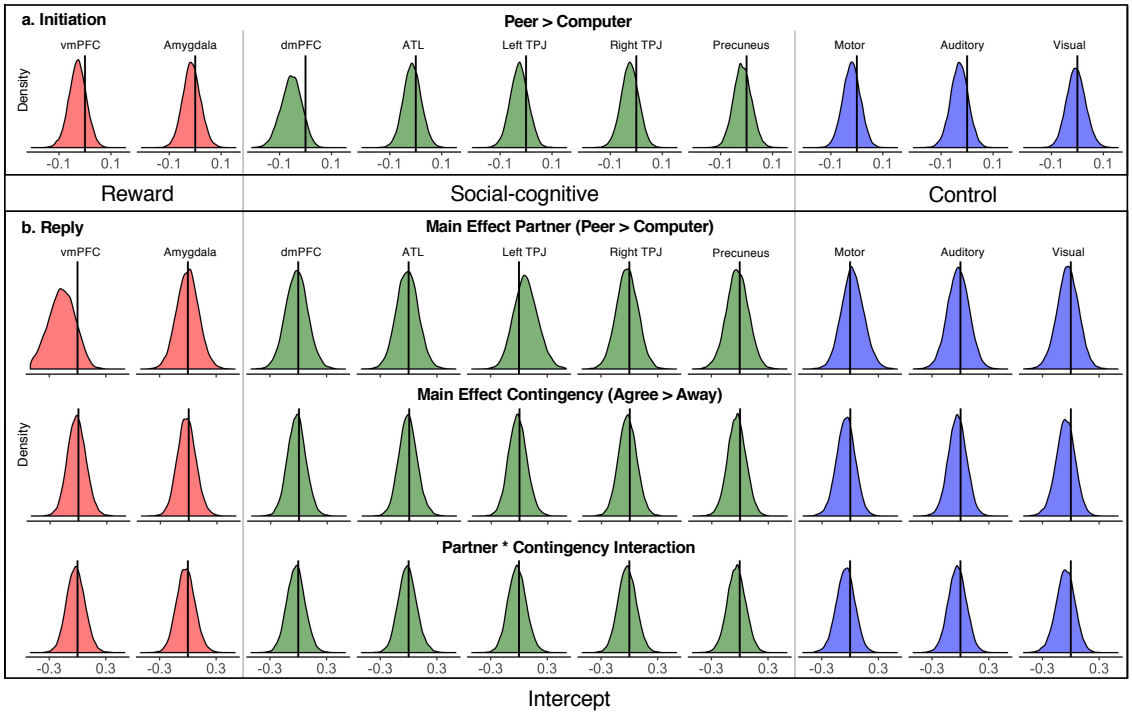


Figure 3.2: Aim 1 main model ROI Results. The posterior distributions surrounding the model intercept for each ROI and contrast are shown for the a) Initiation and b) Reply events. Distribution colors reflect brain systems and the vertical black line on each distribution reflects a contrast value of 0. Distributions that overlap with 0 are interpreted as non-significant effects while distributions highlighted with gray and black boxes denote that the 90% and 95% CIs do not overlap with 0, respectively. The mean, SD, and 95% CI values for each distribution are in Table A.1.

### 3.1.2 Reply Event

During the reply event, participants received a response from their partner that either matched the participant's answer (agree trials; e.g., "Me too!", "Matched"), showed that the partner received the participant's answer but could not respond (away trials; e.g., "I'm away.", "Disconnected"), or did not match the participant's answer. The subsequent analysis will only focus on the agree and away trials. On the post-scan questionnaire, we used participant ratings on the agree questions "How did you feel when the (peer's name) agreed with your answer" / "How did you feel when the computer matched your answer" as an index of a subjective feeling of reward and, for the away questions, "How did you feel when (peer's name) was away and could not respond" / "How did you feel when the computer was disconnected" as an index of subjective response to no reward.

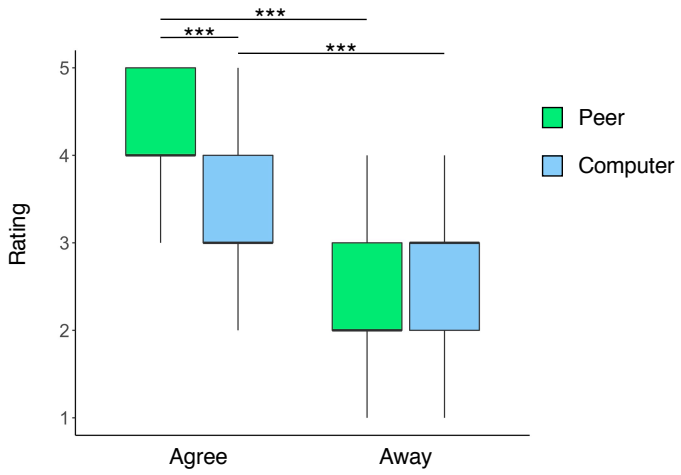


Figure 3.3: Aim 1 reply event behavioral results for NT group. Boxplot of self-report post-scan questionnaire ratings of reward in response to the different reply conditions of interest. ***$p$ <0.001

Using a mixed-effects model to control for within-participant repeated mea-

sures, participants in the NT group reported both greater enjoyment from receiving a response from the peer compared to the computer ($\beta_{peer}$=1.02, 95% CI [0.74,1.29], $t(186)$=7.20, $p$ <0.001) and greater enjoyment during the agree compared to the away responses ($\beta_{agree}$=1.95, 95% CI [1.67,2.23], $t(186)$=13.84, $p$ <0.001). In addition, we observed a statistically significant interaction between partner and response type such that the receipt of the reward (e.g., agree trials) was reported as more rewarding for the peer compared to the computer trials ($\beta_{interaction}$=1.06, 95% CI [0.66,1.46], $t(186)$=5.33, $p$ <0.001) (Figure 3.3).

With respect to VS functional connectivity during the reply events, the posterior distributions for the ROIs within the reward and the social-cognitive systems overlapped with 0, which suggests little evidence that the VS was modulated by modulated by the presence of the peer (i.e., main effect of partner type), receipt of reward (i.e., main effect of reward contingency), or an interaction between partner and contingency type. In addition, we did not detect effects within the control ROIs for the aforementioned contrasts. See Figure 3.2b for the posterior distributions and Table A.1 for their corresponding mean, SD, and 95% CIs. Similarly, exploratory VS to whole brain functional connectivity analysis did not reveal any statistically significant clusters for the either the main effect of partner type, main effect of reward contingency, or partner type by contingency interaction (voxelwise $p$ <0.001, $k$=19, FWE=$p$ <0.05).

Since our main question of interest deals with how a social reward modulates VS functional connectivity, we followed up our previous model to examine the significance of each relevant pairwise reply contrast (i.e., peer agree-away, peer-computer

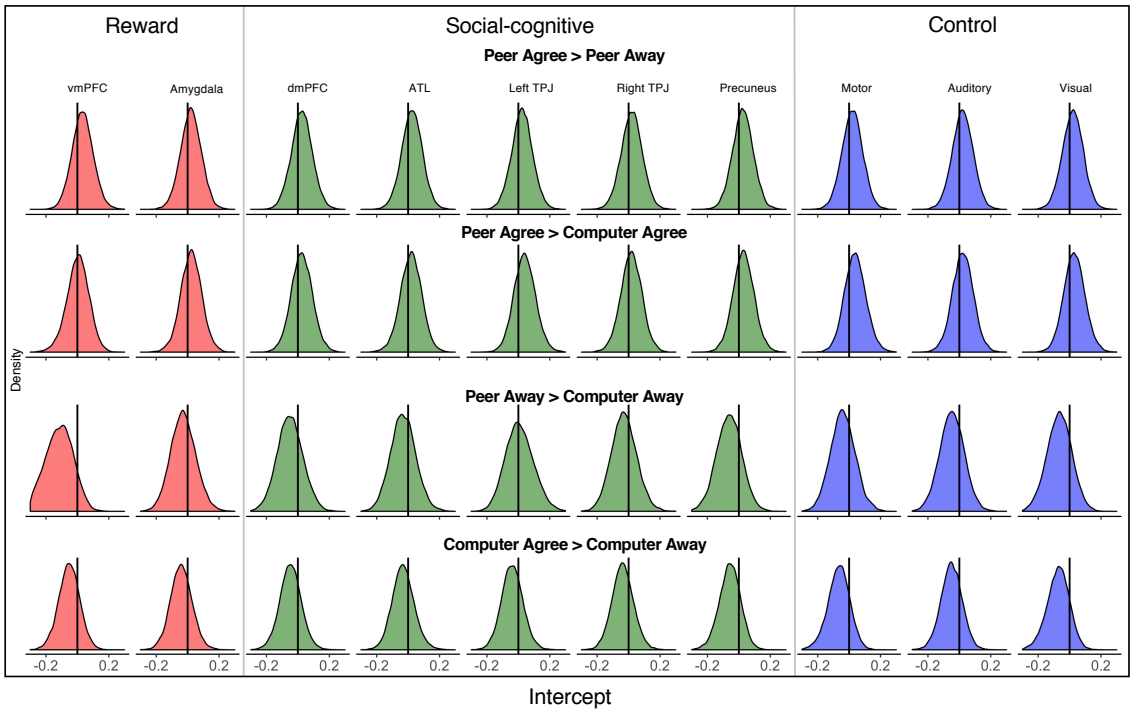


Figure 3.4: Aim 1 pairwise ROI results. The posterior distributions surrounding the model intercept for each ROI are shown for each pairwise reply contrast. Distribution colors reflect brain systems and the vertical black line on each distribution reflects a contrast value of 0. Distributions that overlap with 0 are interpreted as non-significant effects while distributions highlighted with gray and black boxes denote that the 90% and 95% CIs do not overlap with 0, respectively. The mean, SD, and 95% CI values for each distribution are in Table A.2.

agree, peer-computer away, and computer agree-away). For the peer agree-away contrasts (i.e., the receipt of a social reward versus the presence of a social partner), we did not detect an effect within either the reward, social-cognitive, or control ROIs. For the peer-computer agree contrast (i.e., the receipt of a social reward versus a non-social reward), we also did not detect an effect within either the reward, social-cognitive, or control ROIs. For the peer-computer away contrast (i.e., the effect of presence of a social partner), we also did not detect an effect within either the reward, social-cognitive, or control ROIs. And finally, for the computer

agree-away contrast (i.e., the receipt of a non-social reward), we did not detect an effect within either the reward, social-cognitive, or control ROIs. See Figure 3.4 for the posterior distributions and Table A.2 for their corresponding main, SD, and 95% CIs. Similarly, exploratory VS to whole brain functional connectivity analysis did not reveal any statistically significant clusters for any of the pairwise reply contrasts (voxelwise $p$ <0.001, $k$=19, FWE=$p$ <0.05).

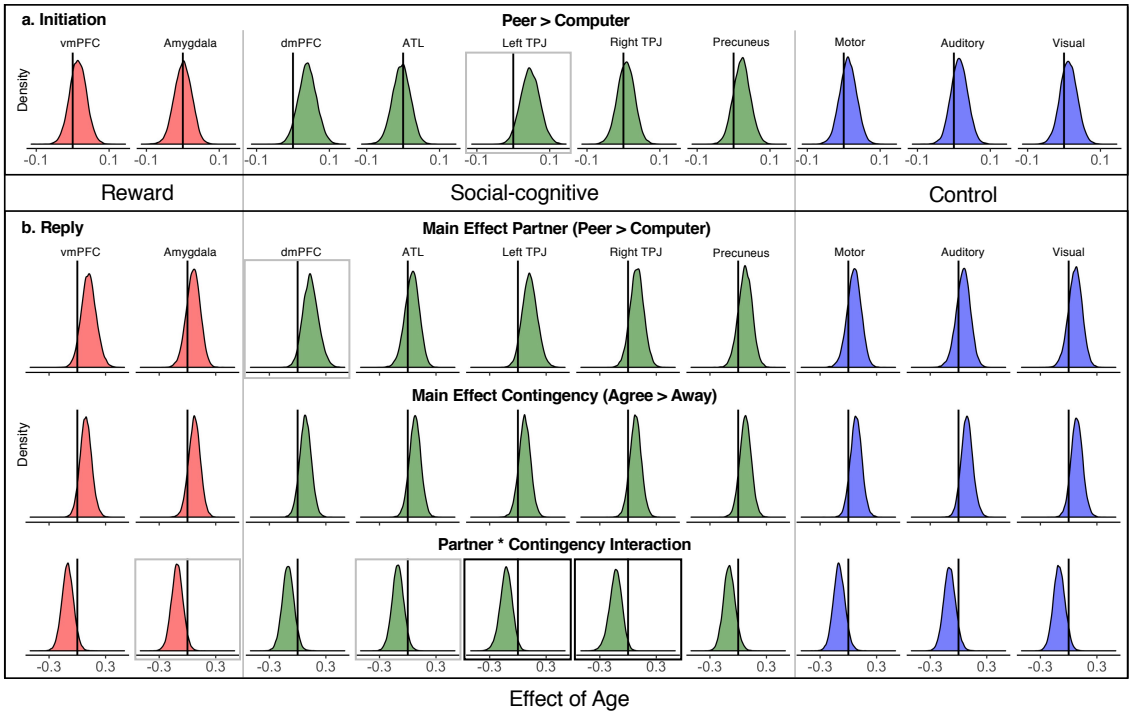


Figure 3.5: Aim 1 main model effect of age ROI results. The posterior distributions surrounding the effect of age for each ROI and contrast are shown for the a) Initiation and b) Reply events. Distribution colors reflect brain systems and the vertical black line on each distribution reflects a contrast value of 0. Distributions that overlap with 0 are interpreted as non-significant effects while distributions highlighted with gray and black boxes denote that the 90% and 95% CIs do not overlap with 0, respectively. The mean, SD, and 95% CI values for each distribution are in Table A.3.

Given that middle childhood is a time of developmental change in both behavior and brain organization, we next examined the effect of age on VS functional

connectivity (Figure 3.5). For the peer-computer initiation contrast, the 90% CI of the posterior distribution surrounding the effect of age within the left TPJ was greater than 0, suggesting some evidence that VS to left TPJ functional connectivity increases sensitivity to engage with a social partner as a function of age. The distributions surrounding the effect of age within the other reward, social-cognitive, and control ROIs all overlapped with 0 (Figure 3.5a). For the main effect of partner reply, we found that the 90% CI for the dmPFC was greater than 0, suggesting some evidence that VS to dmPFC functional connectivity increases sensitivity to a social partner as a function of age. For the main effect of reward contingency, we did not find evidence that any of the reward, social-cognitive, or control ROIs exhibited an effect of age. Finally, for the partner by contingency type interaction, we found that the 90% CI for the effect of age for the amygdala and ATL and the 95% CI for the effect of age for the left and right TPJ were less than 0, suggesting a negative interaction effect. See Figure 3.5b for the distributions main models within the reply event and Table A.3 for their corresponding main, SD, and 95% CIs.

To follow up on the partner type of reward contingency interactions with age seen in Figure 3.5, we then examined the age effects within each pairwise reply contrast (see Figure 3.6 and Table A.4 for corresponding values). We observed that the negative directionality and significant partner by contingency interactions in the amygdala, ATL, and left and right TPJ are driven by both an increase in VS functional connectivity to the peer away compared to the peer agree replies as well as an increase in the computer agree compared to the computer away replies. Exploratory VS to whole brain functional connectivity analysis did not reveal any

statistically significant clusters for the either the main effect of partner type, main effect of reward contingency, partner type by contingency interaction, or any of the pairwise reply contrasts (voxelwise $p$ <0.001, $k$=19, FWE=$p$ <0.05).

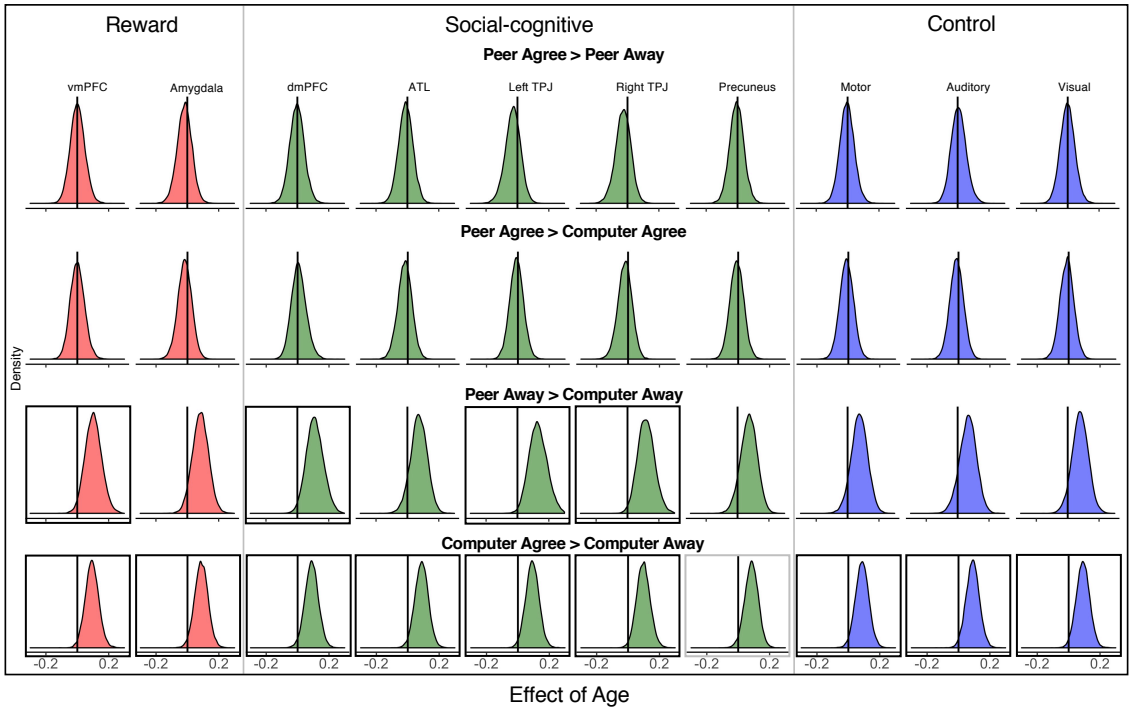


Figure 3.6: Aim 1 reply pairwise effect of age ROI Results. The posterior distributions surrounding the effect of age for each ROI are shown for each pairwise reply contrast. Distribution colors reflect brain systems and the vertical black line on each distribution reflects a contrast value of 0. Distributions that overlap with 0 are interpreted as non-significant effects while distributions highlighted with gray and black boxes denote that the 90% and 95% CIs do not overlap with 0, respectively. The mean, SD, and 95% CI values for each distribution are in Table A.4.

## 3.2 Aim 2: Functional Connectivity in the ASD Compared to NT Group

### 3.2.1 Initiation Event

For the between-group analysis in Aim 2, we used age- and sex- matched NT and ASD groups. As in the previous aim, all participants believed that they were chatting in real-time with a peer during the peer trials as reported on the post-scan questionnaire. Behavioral performance during the Initiation event was similar between groups such we did not observe group differences in how quickly participants responded to the self-relevant prompt ($\beta_{NT}$=-0.10, 95% CI [-0.24 0.03], $t(64)$=-1.45, $p$ =0.15). As in Aim 1, we also observed a similar weak pattern such that participants tended to respond to the peer trials quicker than the computer trials ($\beta_{peer}$=-0.03, 95% CI [-0.07 0.00], $t(60)$=-1.92, $p$ =0.06)(Figure 3.7a). Further, the interaction term in the above model was not statistically significant ($\beta_{interaction}$=0.42, 95% CI [-0.03 0.07], $t(60)$=0.82, $p$ =0.42).

With respect to the post-scan questionnaire, we did not observe a main effect of group affiliation on how motivated participants were to see the response to their answer ($\beta_{NT}$=0.23, 95% CI [-0.33 0.78], $t(103)$=0.79, $p$ =0.43). However, as in Aim 1, we did find evidence that both groups rated greater motivation to see the peer compared to the computer's replies ($\beta_{peer}$=0.84, 95% CI [0.40 1.28], $t(60)$=3.77, $p$ <0.001) (Figure 3.7b). In addition, the interaction term was not statistically significant ($\beta_{interaction}$=0.42, 95% CI [-0.20 1.03], $t(60)$=1.33, $p$ =0.19).

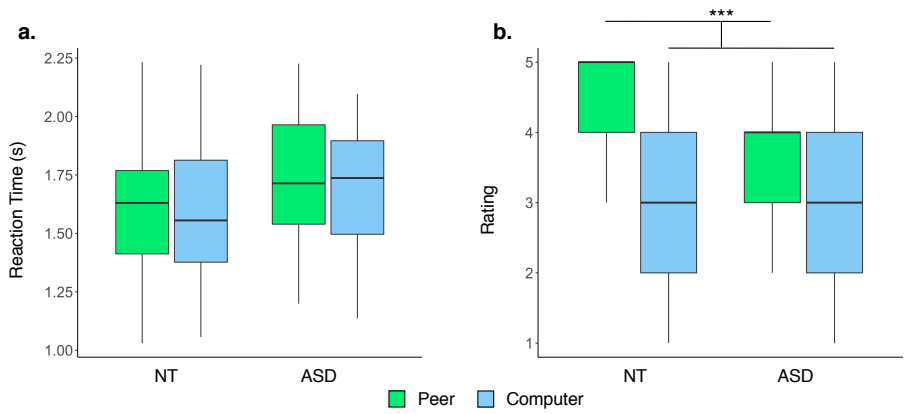


Figure 3.7: Aim 2 Initiation event behavioral results for NT and ASD groups. a) Boxplot of reaction time for both the peer and computer trials. b) Boxplot of self-report post-scan questionnaire ratings of motivation to see each chat partner's response. ***$p$ <0.001

To examine group differences in VS functional connectivity during the Initiation event, we entered all matched-group participant $\beta$ values from the peer-computer initiation contrast from all ROIs into a Bayesian multilevel model. Here our effect of interest is group membership, while also controlling for fixed-effects of participant age, condition-specific head motion, IQ and random effects of ROI and participant. Since we coded the ASD group as 0 and the NT group as 1, we interpret a positive effect of group as a greater contrast $\beta$ value in the NT group whereas a negative group effect suggests a greater contrast $\beta$ value in the ASD group. We did not detect an effect of group on the peer-computer initiation contrast within any of the reward, social-cognitive, or control ROIs (see Figure 3.8a for the posterior distributions for each ROI and Table A.5 for the mean, SD, and 95% CIs surrounding the posterior distribution of the effect of group membership). Similar to our ROI findings, exploratory VS to whole brain functional connectivity analysis did not reveal any statistically significant clusters for the peer-computer initiation con-

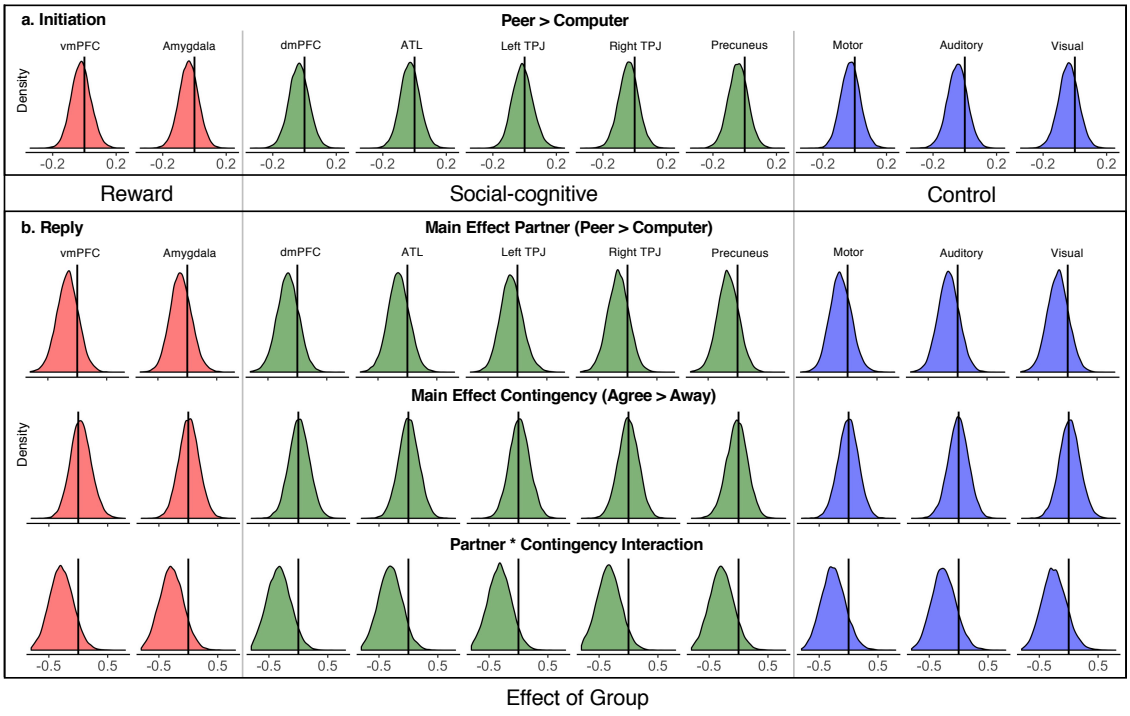


Figure 3.8: Aim 2 main model group ROI results. The posterior distributions surrounding the effect of group membership (NT-ASD) for each ROI and contrast are shown for the a) Initiation and b) Reply events. Distribution colors reflect brain systems and the vertical black line on each distribution reflects a contrast value of 0. Distributions that overlap with 0 are interpreted as non-significant effects while distributions highlighted with gray and black boxes denote that the 90% and 95% CIs do not overlap with 0, respectively. Positive values suggest greater contrast values in the NT group while negative values suggest greater contrast values in the ASD group. The mean, SD, and 95% CI values for each distribution are in Table A.5.

trast (voxelwise $p$ <0.001, $k$=19, FWE=$p$ <0.05). Exploratory VS to whole brain functional connectivity analysis did not reveal any statistically significant clusters (voxelwise $p$ <0.001, $k$=19, FWE=$p$ <0.05).

### 3.2.2 Reply Event

Using a mixed-effects model to control for within-participant repeated measures, we did not detect group differences in how participants in the NT and ASD

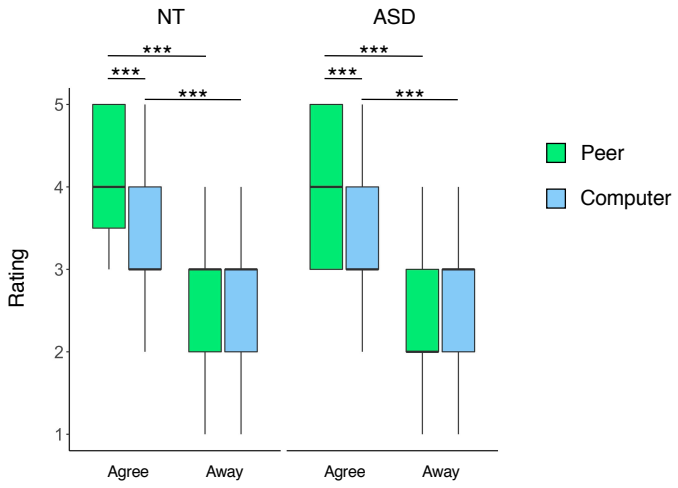


Figure 3.9: Aim 2 Reply event behavioral results for NT and ASD groups. Boxplot of self-report post-scan questionnaire ratings of reward in response to the different reply conditions of interest. ***$p$ <0.001

groups rated their subjective feeling of reward to each of the four reply types of interest ($\beta_{NT}$=0.14, 95% CI [-0.16,0.43], $t(60)$=0.93, $p$ =0.36) or a 3-way group by partner by contingency interaction ($\beta_{interaction}$=0.16, 95% CI [-0.70,1.00], $t(180)$=0.37, $p$ =0.71). Similar to our Aim 1 results, participants in the ASD and NT groups reported both greater enjoyment from receiving a response from the peer compared to the computer ($\beta_{peer}$=0.76, 95% CI [0.46,1.06], $t(183)$=4.97, $p$ <0.001) and greater enjoyment during the agree compared to the away responses ($\beta_{agree}$=1.56, 95% CI [1.27,1.87], $t(183)$=10.26, $p$ <0.001). In addition, within both groups we observed a statistically significant interaction between partner and response type such that the receipt of the reward (e.g., agree trials) was reported as more rewarding for the peer compared to the computer trials ($\beta_{interaction}$=0.85, 95% CI [0.43,1.27], $t(183)$=3.96, $p$ <0.001) (Figure 3.9).

With respect to group differences in VS functional connectivity, we entered

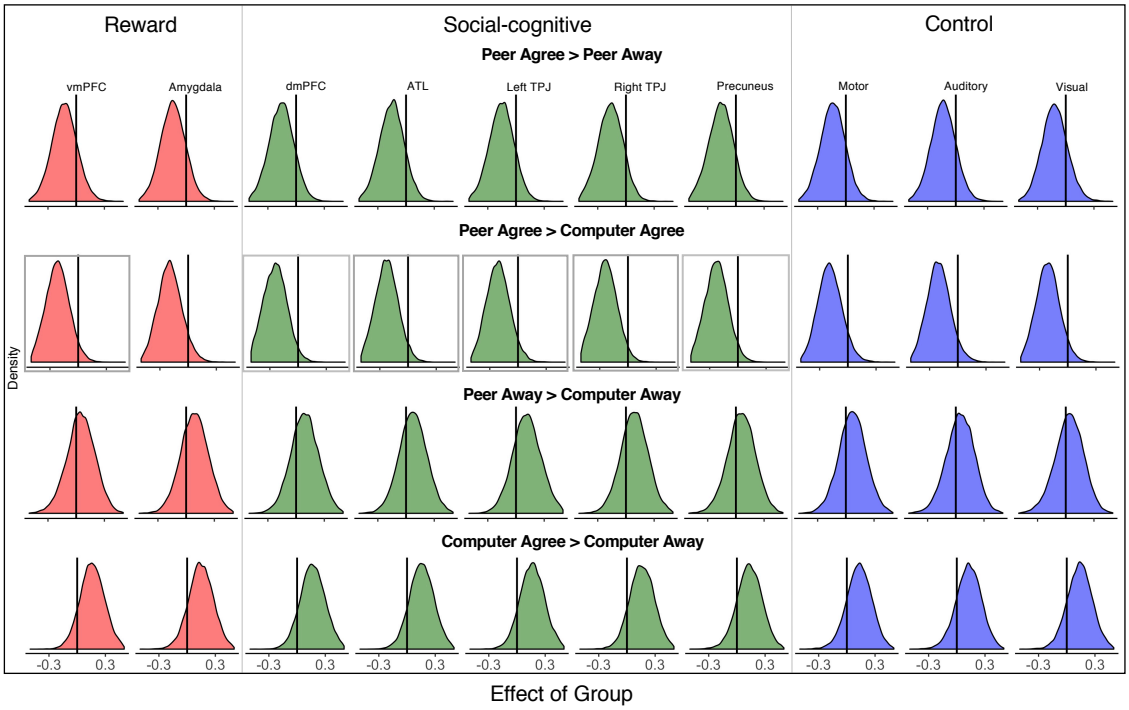


Figure 3.10: Aim 2 reply pairwise group ROI results. The posterior distributions surrounding the effect of group membership (NT-ASD) for each ROI are shown for each pairwise reply contrast. Distribution colors reflect brain systems and the vertical black line on each distribution reflects a contrast value of 0. Distributions that overlap with 0 are interpreted as non-significant effects while distributions highlighted with gray and black boxes denote that the 90% and 95% CIs do not overlap with 0, respectively. Positive values suggest greater contrast values in the NT group while negative values suggest greater contrast values in the ASD group. The mean, SD, and 95% CI values for each distribution are in Table A.6.

contrast $\beta$ values for each of the reply events from each ROI from each participant in a Bayesian multilevel model. As with the Initiation event, our effect of interest here was also group membership while controlling for the fixed-effects of age, condition-specific motion, IQ, and the random effects of ROI and participant. For the main effect of partner and contingency types, as well as their interaction, the posterior distributions surrounding the effect of group membership all overlapped with 0 for all reward, social-cognitive, and control ROIs, suggesting little evidence

for a group effect within these contrasts (see Figure 3.8b and Table A.5 for corresponding values). However, while the 95% confidence interval for the posterior distributions on the effect of group did overlap with 0 for the partner by contingency type interaction, we noticed that all distributions suggested a trending effect such that the interaction contrast was greater in the ASD compared to the NT group. To examine the directionality of this interaction more closely, we ran models for each of the pairwise reply contrasts to examine the effect of group membership. This analysis revealed that the trend toward a group difference in the interaction contrast is driven primarily by greater VS functional connectivity in the peer compared to the computer agree trials in the ASD group within the vmPFC, ATL, dmPFC, left and right TPJ, precuneus, and visual ROIs (see Figure 3.10 and Table A.6). Exploratory VS to whole brain functional connectivity analysis did not reveal any statistically significant clusters for the either the main effect of partner type, main effect of reward contingency, partner type by contingency interaction, or any of the pairwise reply contrasts (voxelwise $p$ <0.001, $k$=19, FWE=$p$ <0.05).

Given our hypotheses regarding age-related differences, we then conducted an analysis that examine the effect of age on VS functional connectivity within the ASD group separately (since the effect of age in the NT group was examined in Aim 1) (see Figure 3.11 and Table A.7 for corresponding values). Since our ASD sample (N=31) is much smaller than our full NT sample, we exercise restraint in the interpretation of these results given that we do not have sufficient power to detect individual differences. For the peer-computer initiation contrast, we did not detect any effect of age on VS functional connectivity (Figure 3.11a). For the main effect of

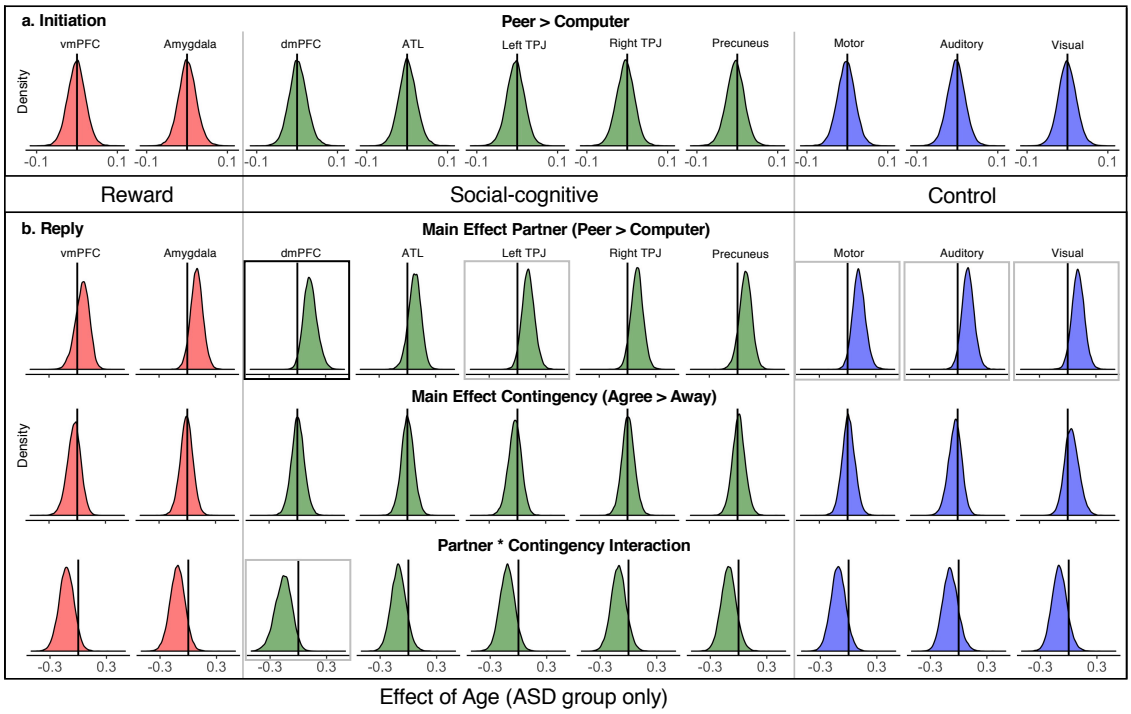


Figure 3.11: Aim 2 main model effect of age ASD ROI results. The posterior distributions surrounding the effect of age for each ROI and contrast are shown for the a) Initiation and b) Reply events. Distribution colors reflect brain systems and the vertical black line on each distribution reflects a contrast value of 0. Distributions that overlap with 0 are interpreted as non-significant effects while distributions highlighted with gray and black boxes denote that the 90% and 95% CIs do not overlap with 0, respectively. The mean, SD, and 95% CI values for each distribution are in Table A.7.

partner type, the 95% CI of the posterior distribution surrounding the effect of age was greater than 0 in the dmPFC, whereas the 90% CI was greater than 0 in the left TPJ and the three control ROIs (motor, auditory, and visual). Finally, the 90% CI was less than 0 for the interaction term for the partner type by reward contingency interaction (Figure 3.11b).

The main model analysis was followed by an examination of the effect of age on VS functional connectivity within each of the pairwise reply contrasts (see Figure 3.12 and Table A.8 for corresponding values). We found that VS functional

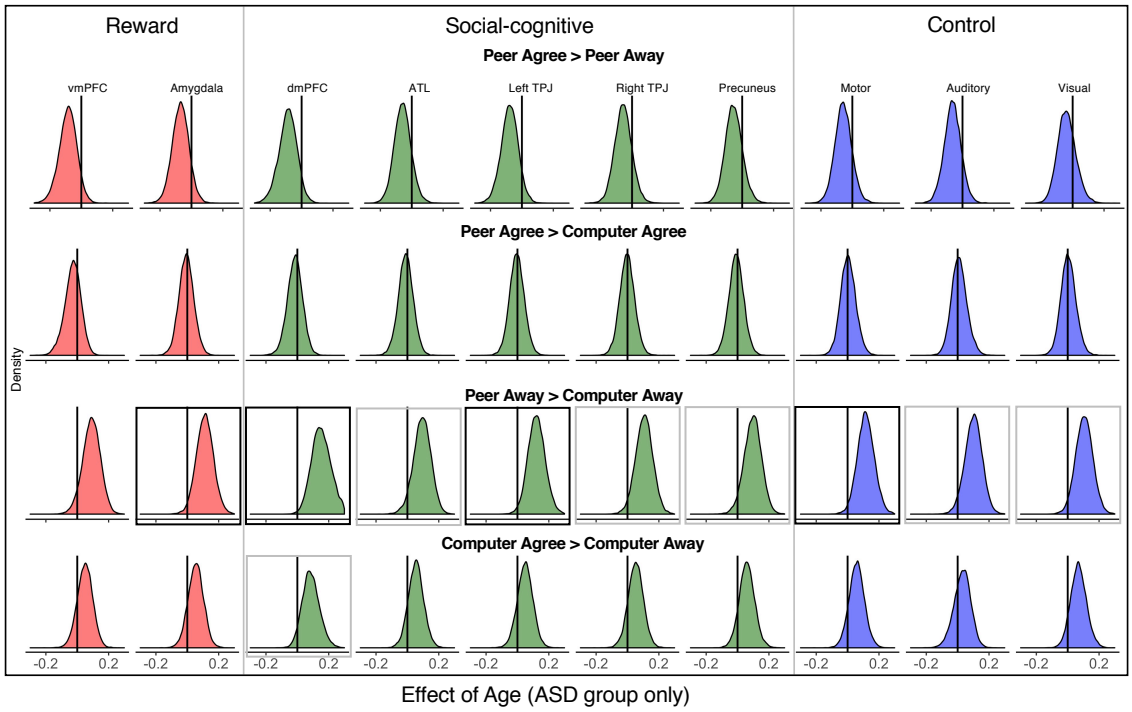


Figure 3.12: Aim 2 reply pairwise effect of age ASD ROI results. The posterior distributions surrounding the effect of age for each ROI are shown for each pairwise reply contrast. Distribution colors reflect brain systems and the vertical black line on each distribution reflects a contrast value of 0. Distributions that overlap with 0 are interpreted as non-significant effects while distributions highlighted with gray and black boxes denote that the 90% and 95% CIs do not overlap with 0, respectively. The mean, SD, and 95% CI values for each distribution are in Table A.8.

connectivity increased as a function of age for the peer-computer away contrast within the amygdala, dmPFC, left TPJ, and motor ROIs (95% CI) and the ATL, right TPJ, precuneus, auditory, and visual ROIs (90% CI). In addition, the 90% CI within the dmPFC for the computer agree-away contrast was greater than 0. Exploratory VS to whole brain functional connectivity analysis did not reveal any statistically significant clusters for the either the main effect of partner type, main effect of reward contingency, partner type by contingency interaction, or any of the pairwise reply contrasts (voxelwise $p$ <0.001, $k$=19, FWE=$p$ <0.05).

## 3.3 Aim 3: Functional Connectivity and Individual Differences.

### 3.3.1 Post Test Ratings

We next examined how VS functional connectivity was modulated by individual differences in participant's subjective reports of the motivation to engage with each chat partner as well as individual differences in autistic traits. For this analysis we created a behavioral contrast score using the relevant post test ratings for each functional connectivity contrast. To examine the effect of post test reports of social motivation, we subtracted the post scan ratings for "How much did you want to see (peer's name)'s response to your question?" from the question "How much did you want to see the computer's answer to your question?" to create a peer-computer behavioral contrast. We then used this behavioral contrast to predict peer-computer initiation functional connectivity while controlling for fixed effects of age, condition-specific motion, and IQ as well as the random effects of participant and ROI. The posterior distribution surrounding the effect of the behavioral contrast for all reward, social-cognitive, and control regions overlapped with 0, suggesting little evidence for an effect (see Figure 3.13a and Table A.9 for corresponding values).

For the reply event, we created behavioral contrasts from the questions "How did you feel when (peer's name) agreed with your answer?" (peer agree), "How did you feel when (peer's name) was away and could not respond?" (peer away), "How did you feel when the computer matched your response?" (computer agree), and "How did you feel when the computer was disconnected?" (computer away). For

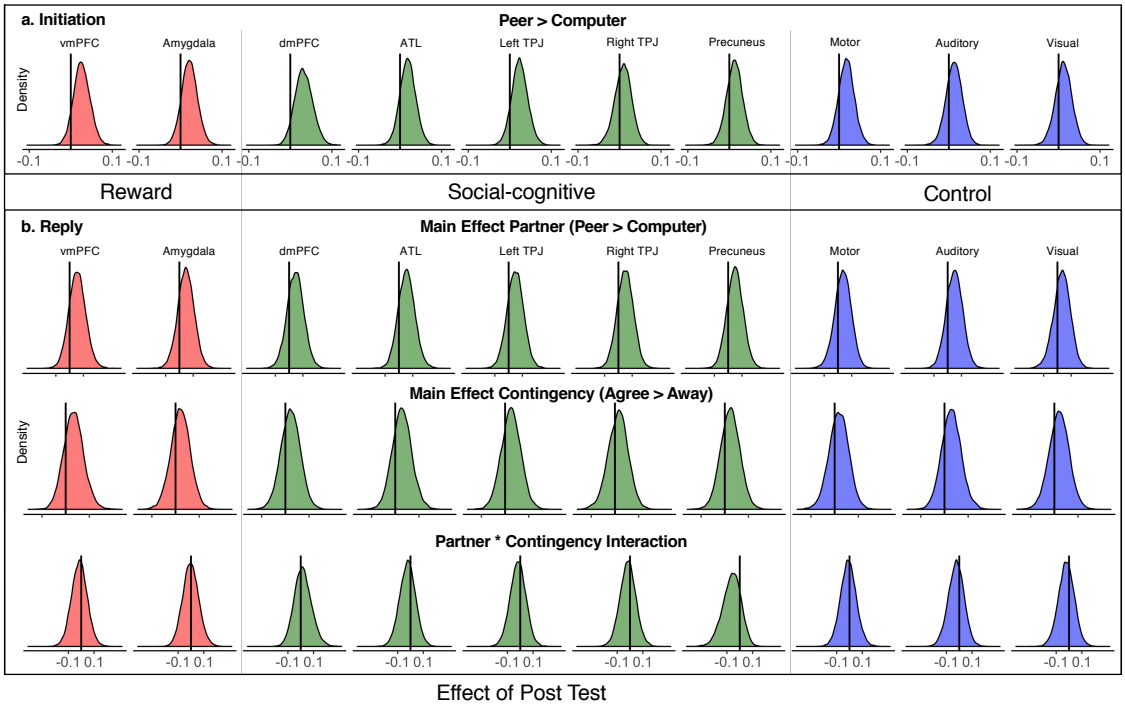


Figure 3.13: Aim 3 main model post test ROI results. The posterior distributions surrounding the effect of post test ratings for each ROI and contrast are shown for the a) Initiation and b) Reply events. Distribution colors reflect brain systems and the vertical black line on each distribution reflects a contrast value of 0. Distributions that overlap with 0 are interpreted as non-significant effects while distributions highlighted with gray and black boxes denote that the 90% and 95% CIs do not overlap with 0, respectively. The mean, SD, and 95% CI values for each distribution are in Table A.9.

the main effect of partner we created a behavioral contrast as defined by (peer agree + peer away) - (computer agree + computer away). For the main effect of contingency we created a behavioral contrast as defined by (peer agree + computer away) - (peer away + computer away). And for the interaction term we created a behavioral contrast as defined by (peer agree - peer away) - (computer agree - computer away). We did not detect any significant effects of the post test behavioral contrasts on the VS functional connectivity contrasts (see Figure 3.13b and Table A.9 for corresponding values). In addition, we followed this analysis up to examine the effects of

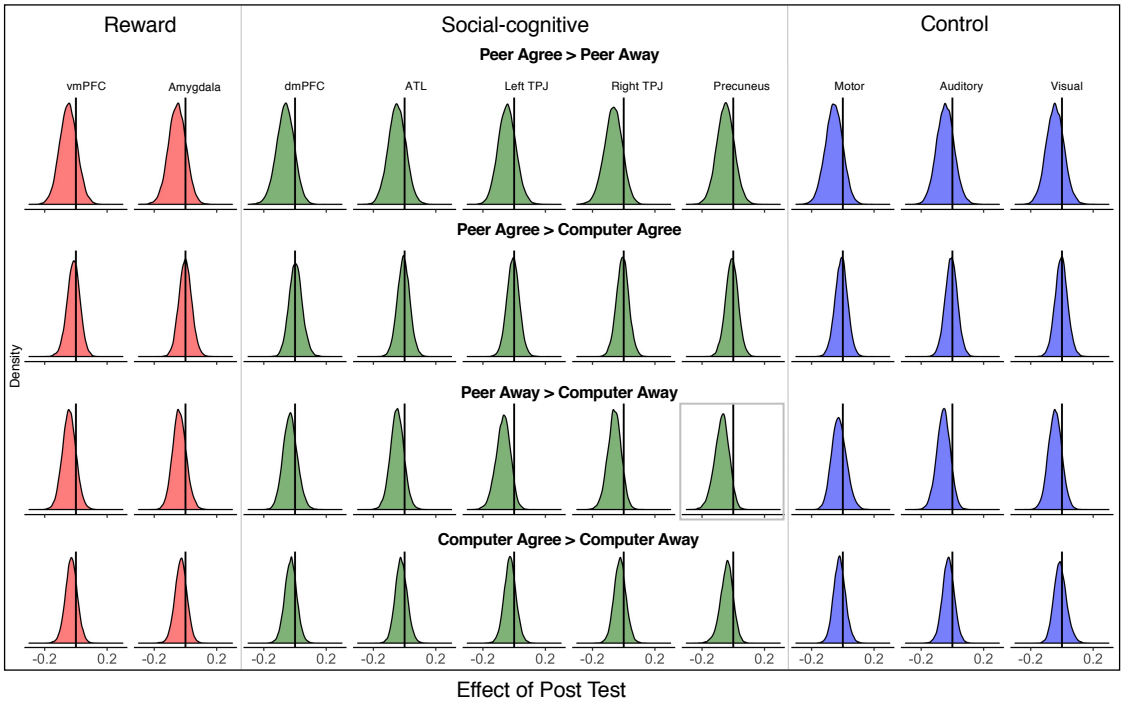


Figure 3.14: Aim 3 reply pairwise post test ROI results. The posterior distributions surrounding the effect of post test ratings for each ROI are shown for each pairwise reply contrast. Distribution colors reflect brain systems and the vertical black line on each distribution reflects a contrast value of 0. Distributions that overlap with 0 are interpreted as non-significant effects while distributions highlighted with gray and black boxes denote that the 90% and 95% CIs do not overlap with 0, respectively. The mean, SD, and 95% CI values for each distribution are in Table A.10.

the post test behavioral contrasts on the pairwise reply VS functional connectivity contrasts. Only one marginal effect was seen (CI 90% less than 0) in the precuneus for the peer-computer away contrast (see Figure 3.14 and Table A.10 for corresponding values). Exploratory VS to whole brain functional connectivity analysis did not reveal any statistically significant clusters for the either the main effect of partner type, main effect of reward contingency, partner type by contingency interaction, or the pairwise reply contrasts (voxelwise $p$ <0.001, $k$=19, FWE=$p$ <0.05).

### 3.3.2 Social Responsiveness Scale

To examine the effect of individual differences in autistic traits on VS functional connectivity, we used scores from the parent report SRS questionnaire (Constantino & Todd, 2003). We first used the SRS social motivation sub-scale to predict the peer-computer initiation functional connectivity contrast, while controlling for fixed effects of age, condition-specific motion, and IQ as well as the random effects of participant and ROI. In this model, we detected that the 90% CIs for the precuneus, auditory, and visual ROIs were greater than 0, suggesting some evidence that greater social motivation on the SRS predicted greater VS functional connectivity in these ROIs for the peer compared to the computer initiation event (see Figure 3.15a and Table A.11 for corresponding values). Then, for the main model reply events, we used the total raw score on the SRS as an index of autistic traits. In this analysis the posterior distributions surrounding the effect of SRS on functional connectivity were non-significant in all ROIs for the main effect of partner, main effect of contingency, and the partner type by reward contingency interaction (see Figure 3.15b and Table A.11 for corresponding values).

In addition, we followed this analysis up to examine the effects of the SRS total raw score on the pairwise reply VS functional connectivity contrasts. Here, we did not observe an effect of SRS scores on any of the pairwise functional connectivity contrasts (see Figure 3.16 and Table A.12 for corresponding values). Similarly, exploratory VS to whole brain functional connectivity analysis did not reveal any statistically significant clusters for the either the main effect of partner type, main

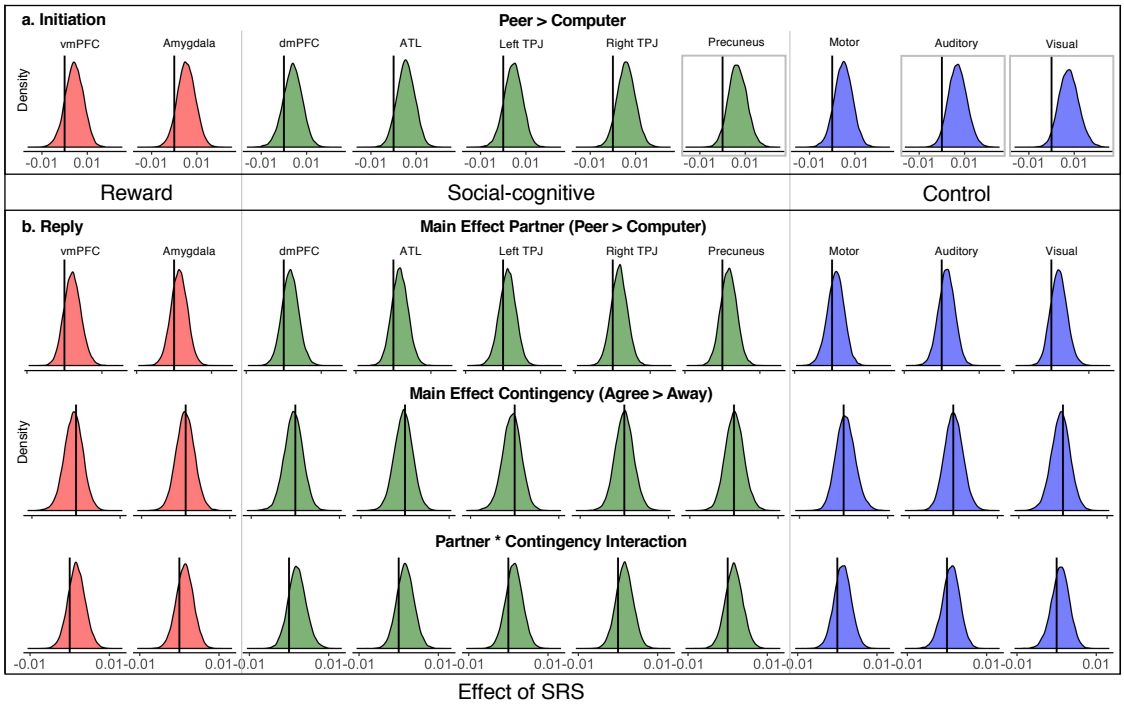


Figure 3.15: Aim 3 main model SRS ROI results. The posterior distributions surrounding the effect of SRS for each ROI and contrast are shown for the a) Initiation and b) Reply events. Distribution colors reflect brain systems and the vertical black line on each distribution reflects a contrast value of 0. Distributions that overlap with 0 are interpreted as non-significant effects while distributions highlighted with gray and black boxes denote that the 90% and 95% CIs do not overlap with 0, respectively. The mean, SD, and 95% CI values for each distribution are in Table A.11.

effect of reward contingency, partner type by contingency interaction, or the pairwise reply contrasts (voxelwise $p$ <0.001, $k$=19, FWE=$p$ <0.05). Exploratory VS to whole brain functional connectivity analysis did not reveal any statistically significant clusters for the either the main effect of partner type, main effect of reward contingency, partner type by contingency interaction, or any of the pairwise reply contrasts (voxelwise $p$ <0.001, $k$=19, FWE=$p$ <0.05).

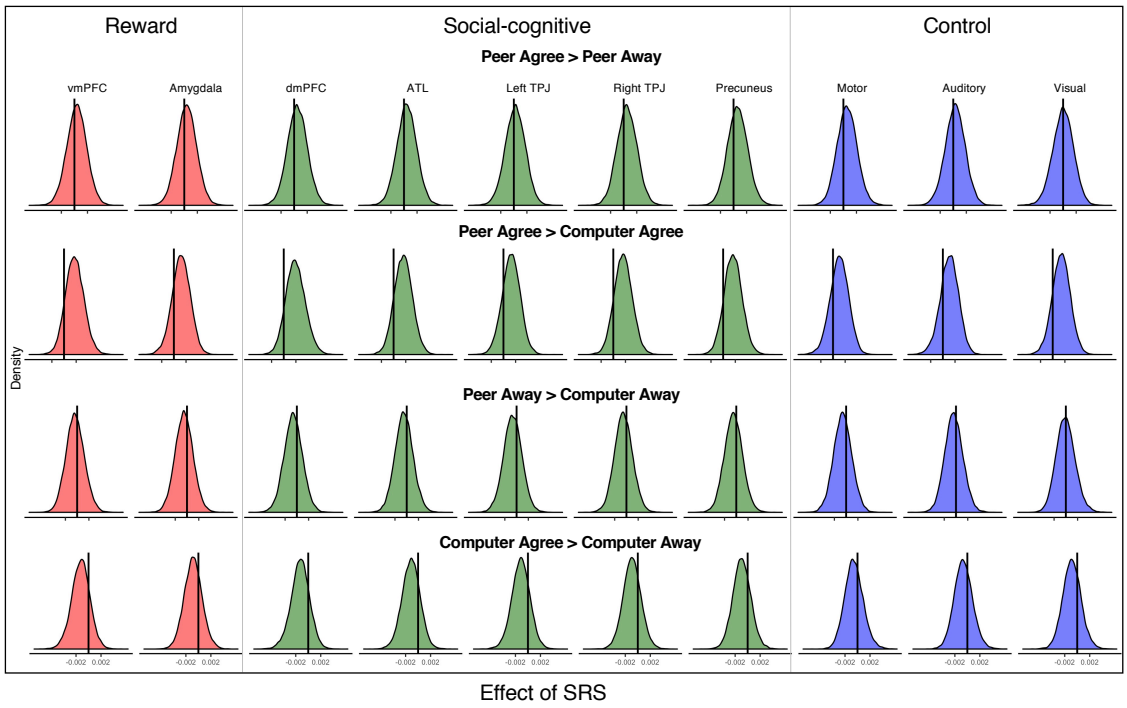


Figure 3.16: Aim 3 reply pairwise SRS ROI results. The posterior distributions surrounding the effect of SRS for each ROI are shown for each pairwise reply contrast. Distribution colors reflect brain systems and the vertical black line on each distribution reflects a contrast value of 0. Distributions that overlap with 0 are interpreted as non-significant effects while distributions highlighted with gray and black boxes denote that the 90% and 95% CIs do not overlap with 0, respectively. The mean, SD, and 95% CI values for each distribution are in Table A.12.

# Chapter 4: Discussion

The purpose of this dissertation was to examine the functional relationship between the ventral striatum (VS) and regions of the reward and social-cognitive brain systems while participants engaged in a real-time social interaction. We use a novel Bayesian multilevel modeling method (G. Chen et al., 2019) to efficiently infer our effects-of-interest while removing the classic issues surrounding multiple comparisons in neuroimaging data. In Aim 1, we sought to characterize VS functional connectivity while participants shared self-relevant information about themselves with a peer and during the receipt of a social reward within a sample of child participants who are neurotypical (NT). In Aim 2, we examined group differences between a sample of participants diagnosed with autism spectrum disorder (ASD) and an age-, sex-, and IQ-matched NT sample (N = 31 in each group). Finally, in Aim 3 we removed the ASD and NT group distinction and took a dimensionality perspective through examining VS functional connectivity as a function of participant's subjective reports of social motivation and social reward, as well as parent-report of participant autistic traits within the entire sample.

Overall, while we found some limited evidence that the VS is modulated by a rewarding social interaction, our findings largely did not support our initial hypothe-

ses. We did not find evidence in the NT group that sharing self-relevant information with a peer or that the receipt of an interactive social reward modulated functional connectivity between the VS and other regions of the reward and social-cognitive systems. We also observed that VS functional connectivity increased as a function of age within the trials where the peer could not respond (peer-away) and the trials where the computer matched the participant's response (computer agree), both of which are inconsistent with the extended common currency framework on which our hypotheses are grounded (Ruff & Fehr, 2014). With respect to group differences between the ASD and NT groups, we found that the ASD group exhibited greater VS functional connectivity to a social reward compared to the NT group within regions of both the reward and social-cognitive systems, a finding that may be inconsistent with the hypothesis that those with ASD may experience a blunting in reward response to social rewards (Chevallier et al., 2012). Finally, using a dimensional approach, we did not find that individual differences in subjective report of social motivation or social reward, as well as autistic traits modulated VS functional connectivity during either phases of our task.

## 4.1 Extended Common Currency Schema

The extended common currency schema posits that higher-order regions of the social brain (e.g., TPJ, dmPFC, ATL, precuneus) will exert influence onto the domain-general value representation system (e.g., VS, vmPFC, amygdala) during the processing of rewarding social stimuli (Ruff & Fehr, 2014). While the foun-

dation of this schema rests on the both the similarity in neural resources used for processing social and non-social rewards within regions of the value representation system (Chavez & Heatherton, 2015; Wake & Izuma, 2017) and the activation of regions implicated in social processing during social rewards (Morishima et al., 2012; Nicolle et al., 2012; van den Bos et al., 2013), recent work has also begun to examine the nature of this influence using functional connectivity methods. This limited literature suggests that regions implicated in reward and social-cognitive processing become integrated when participants pay money to view attractive faces (Smith et al., 2014), during a socially-mediated auction (van den Bos et al., 2013), and while participants made charitable donations (Hare et al., 2010; Janowski et al., 2013).

In the current study we found that both sharing self-relevant information with a social partner and the receipt of a real-time social reward did not modulate reward-to-social-cognitive system functional connectivity in either our NT or ASD samples. While our results are inconsistent with the predictions of the extended common currency schema, all aforementioned studies of connectivity find greater connectivity between reward and social regions within the context of tasks that involve both monetary as well as social processing (Hare et al., 2010; Janowski et al., 2013; Smith et al., 2014; van den Bos et al., 2013). Thus, one possible explanation for the current results is that our task did not involve monetary processing in any capacity. Although previous work has shown that sharing self-relevant information is intrinsically rewarding (Tamir & Mitchell, 2012; Wagner et al., 2015) and that both interactive (Warnell et al., 2017) and non-interactive social rewards (see Bottini, 2018 for review) are associated with greater activation in regions implicated in reward and

social-cognitive processing, perhaps the reward-to-social-cognitive functional connectivity seen in previous studies is driven by the fact that the social processing tasks that included a monetary component.

While the current study is the first to examine functional connectivity between regions of the reward and social-cognitive brain systems within a non-monetary social reward task, our task cannot address the possible independent or emergent effects associated with monetary, social, and social monetary tasks. To precisely evaluate the extended common currency schema, future work should seek to disentangle the relative contributions and interactions between monetary and social rewards. Further, the previous work that examines functional connectivity between reward and social regions typically examine connectivity between the vmPFC, not the VS (Hare et al., 2010; Janowski et al., 2013; Smith et al., 2014; van den Bos et al., 2013). Only one study has examined connectivity between the VS specifically and regions of the social brain (van den Bos et al., 2013). Thus, given the vmPFC's role in the conversion of a reward stimulus into a subjective hedonic value (Levy & Glimcher, 2012), perhaps greater reward-to-social-cognitive connectivity would be seen in the interactive chat task using the vmPFC as a seed region, whereas reward processing in the VS may be confounded with the VS's role in salience detection.

## 4.2 The Function of the Ventral Striatum

The VS is typically cited as a hub of reward (Haber & Knutson, 2010; Sesack & Grace, 2010) and motivational processing (Sescousse et al., 2015) whose response

signals the presence of a rewarding stimuli in one's environment (Levy & Glimcher, 2012). Further, response in the VS parametrically increases as a function of subjective reward value (see Levy & Glimcher, 2012 and Sescousse et al., 2015 for reviews). However most studies cannot disentangle whether response in the VS is due to reward value per se or the general salience of rewarding stimuli (Bossong & Kahn, 2016; Jensen et al., 2007). Indeed, the VS has also been shown to encode the salience of both monetary losses as well as gains (Cooper & Knutson, 2008; Jensen et al., 2007), suggesting that response in this region may not be specific to only positive aspects of motivation and/or reward processing. Consistent with this view, one recent meta-analysis found that the VS was associated with psychological terms such as 'incentive', 'success', 'rewards', as well as 'losses' (Pauli et al., 2016). With respect to social stimuli, the VS responds to salient changes in static social stimuli above the social reward of seeing a smiling face (Schmidt et al., 2018), as well as to both social reward and avoidance of social punishment (Kohls et al., 2013). Thus, while the common currency schema (Ruff & Fehr, 2014) predicts an increase in the response in and/or functional connectivity with the domain-general valuation regions to rewarding social stimuli, the VS's role within the brain's salience-detection system cannot be ignored.

In the current study we did not find evidence for increased VS connectivity with other regions of the reward and social-cognitive system during the receipt of an interactive social reward. However, while we hypothesized that a positive response from a peer would elicit greater VS functional connectivity, it is possible that the salience of the other response outcomes obscured the relative effect of the social

reward. For example, in the peer agree-away contrast the peer-agree and peer-away conditions may have both been equally salient such that while the receipt of a social reward may be salient, the unexpected absence of a social partner is salient as well. In our lab's activation analysis of the current task, greater activation was seen in regions implicated in social cognition (e.g., TPJ, ATL) during the peer away compared to the computer away responses (Warnell et al., 2017). Thus, if the VS is involved in salience detection and both peer responses are salient (but in different ways) then we may not see differences in VS functional connectivity between the peer agree and peer away responses.

Further, with respect to the computer responses, our task may have a similar confound such that the computer agree trials could be salient due to the participants receiving a "Matched!" response whereas the computer away trials may be salient because participants are surprised by the fact that the computers in a hi-tech MRI facility would be "Disconnected". Future work should differentiate social salience versus social reward in evaluating the extended common currency schema, perhaps through subjective reports of each construct. While the current study sought to examine the relationship between subjective reports of the feeling of reward, our post-scan questions were not structured to disentangle reward from salience.

## 4.3 Increased Connectivity with Age

While our results did not provide evidence that functional connectivity between the VS and regions within the reward and social-cognitive systems increased

while sharing self-relevant information with a peer and during the receipt of an interactive social reward at the group level, we did find evidence of age-related differences in VS connectivity in both the NT and ASD groups. In the NT group, we found that connectivity between the VS and the left TPJ increased as a function of age while sharing self-relevant information with a peer. This finding provides some evidence that the social-to-reward system coupling outlined in the extended common currency schema (Ruff & Fehr, 2014) may increase with age. Further, age-related increases in activation have been seen in regions within regions of the social brain in response to an interactive social partner (Warnell et al., 2017), as well as neural specialization for mental state representation (Gweon et al., 2012; Saxe et al., 2009). One possible explanation is that as children's social worlds expand (Carr, 2017), the intrinsic reward of sharing self-relevant information (Tamir & Mitchell, 2012) becomes coupled with one's tracking of a social partner's mental state. While the previous finding is consistent with the extended common currency framework, our age-related findings during the reply event were counter to what we predicted.

In both the NT and the ASD groups, our results provide evidence that VS functional connectivity increased with age within regions of both the reward and social-cognitive brain systems during the peer away compared to the computer away replies While these findings are contrary to our hypotheses, they are consistent with the aforementioned view of the VS's function in salience detection. Previous activation analysis suggests that the absence of a social partner increases response in regions of the social brain (Warnell et al., 2017) and that a social context modulates age-related differences in both the VS and dmPFC during a gambling task (Braams

et al., 2014). Thus, in terms of greater connectivity during the peer away compared to the computer away responses, one interpretation is that the VS could be signaling the salience of the absence of the social partner while regions implicated in social-cognitive processing are tracking the mental state of the absent partner.

Further, while we found an increase in VS connectivity within the reward regions (i.e., vmPFC and amygdala) with age during the computer agree compared to the computer away replies, we also found age-related increases within the social-cognitive and control regions as well. In terms of the reward system connectivity, this could be consistent with previous work that suggests that response within the VS increases in reward sensitivity with age (Schreuders et al., 2018), however, given that we observed an increase in connectivity with age in all regions including the control regions, we cannot be confident in the specificity of this effect.

## 4.4 Evaluation of the Social Motivation Theory of ASD

The social motivation theory predicts atypical response within the reward system to social rewards in those with ASD (Chevallier et al., 2012) and, taken together with the extended common currency schema (Ruff & Fehr, 2014), atypical social reward processing in ASD may be indexed through differences in reward-to-social-cognitive system functional connectivity However, we did not find evidence for this hypothesis in our results. Our findings do not suggest that functional connectivity was less (relative to NT controls) while participants with ASD shared self-relevant information with a peer or during the receipt of an interactive social

reward. Further, we did not find that VS connectivity decreased as a function of autistic traits. We did, on the other hand, find contrary evidence such that the VS exhibited increased functional connectivity with reward and social-cognitive regions during a social reward (i.e., peer-computer agree) in the ASD group. While this suggests greater integration of the reward and social-cognitive systems during a social reward in ASD, there were no group differences in self-report feelings of reward in response to the peer agree compared to the computer agree reply.

Our results are consistent through the lens of recent criticism of the social motivation theory, which suggests that those with ASD do not exhibit blunted social motivation or social reward (Jaswal & Akhtar, 2018). This critical work views the social motivation theory as an artifact of the field's neurotypical perspective on social reward processing and that there may be alternative interpretations of the classic metrics used to index social motivation and reward. The assumption behind many behavioral measures, such as eye contact and social approach, are that they index one's social interest, social motivation, and social reward, however, based on autistic testimony, this assumption is demonstrably false (Jaswal & Akhtar, 2018). For example, those with ASD may make less eye contact because they are processing a social interaction differently compared to neurotypical individuals (e.g., focusing more on speech rather than eyes)(Moriuchi et al., 2017; Rice et al., 2012), not because they are less motivated to interact or less rewarded from the interaction (Jaswal & Akhtar, 2018).

Taking another perspective, while the task in the current study involves a novel and interactive social interaction, it is possible that the features of the task are such

that those with ASD (or higher autisitc traits) may not show behavioral or neural blunting in response to a social partner. Social deficits in ASD are often exacerbated by real-world, naturalistic contexts (Schilbach et al., 2013) and are often observed through atypical use of speech, gesture, and/or eye contact (American Psychiatric Association, 2013; Jaswal & Akhtar, 2018). However in the current study, the interactive chat task is text-based and did not involve face-to-face communication. Thus, it is possible that the current task is actually a social interaction stripped of the features that cause those with ASD difficulty. Consistent with this interpretation, those with ASD often report that social interactions through abstracted, text-based media (such as the Internet) are more comfortable than in-person interactions (Mazurek, 2013; Penny & P, 2009; Ward et al., 2018).

## 4.5 Social Reward Processing and Timescale

Finally, to fully appreciate the how multiple brain systems work together to processes social motivation and social reward, researchers must examine the nature of both within- and between-system dynamics. The cerebral cortex is organized as a complex network that processes information across multiple timescales (Hasson et al., 2008; Kiebel et al., 2008). For example, primary sensory cortices respond to rapid changes in incoming sensory information whereas higher-order cortices may accumulate information over longer timescales (e.g., from seconds to minutes to hours prior) (J. Chen et al., 2016; Hasson et al., 2008; Honey et al., 2012). Previous work has found that regions sensitive to information presented at long timescales

are topographically similar to the same regions implicated in the default mode network and social-cognitive processing (e.g., TPJ, precuneus, dmPFC) (J. Chen et al., 2016; Hasson et al., 2010). However, while the relationship between cortical temporal hierarchy and social-cognitive processing has yet to be characterized in the brain (Moraczewski et al., in prep), understanding other people in the real world certainly requires the integration of information across multiple timescales (Hasson & Honey, 2012; Koster-Hale & Saxe, 2013; Zaki & Ochsner, 2009). Thus, to represent a potentially rewarding social interaction one must integrate incoming sensory information (e.g., speech, facial expression) with knowledge of the context of the interaction and one's history (or lack thereof) with their social partner (e.g., long timescale information).

While determining the nature, mechanism, and psychological function of these diverse neural timescales is an active area of research (Chaudhuri et al., 2015; Deco et al., 2019; Hasson et al., 2015; Himberger et al., 2018; Honey et al., 2012; Murray et al., 2014; Watanabe et al., 2019), much of this work focuses solely on the functional organization of the cortex, which ignores the contributions of subcortical structures to overall brain dynamics (Bell & Shine, 2016; J. Liu et al., 2015). With respect to reward processing and neural timescale, little is known regarding how timescale informs VS response to rewards in humans. In order to detect rapid alterations in the reward and/or salience landscape, the VS must respond to stimuli at very quick timescales (van der Meer et al., 2010), though previous work suggests that not all stimuli are equal across time. One study found that, as rats became more proficient and a task becomes more predictable, rapid VS response to rewards

diminished (van der Meer & Redish, 2009). However, while the correlation between electrocortical activity (using EEG) and the BOLD signal in the VS has been established in humans (Carlson et al., 2011), less is known regarding the relationship between VS BOLD activation, reward processing, and timescale. Further, previous work suggests differential phasic relationships between cortical and subcortical circuits (Y. Liu et al., 1999; J. Liu et al., 2015) and that this dynamic spatio-temporal organization of fast and slow timescales may enable complex cognitive phenomena (Déli et al., 2017).

In the current study, our context-dependent functional connectivity measures assume that regional co-activation occurs within the same timescale for all regions. Thus, a possible artifact of the generalized psychophysiological interaction method is that the interaction terms are defined by setting all time points that do not occur within a certain post-stimulus window to 0 (McLaren et al., 2012). Our current methods cannot characterize nuanced dynamics between the VS and regions that may be accumulating information across longer timescales. For example, if the VS is responding to transient changes in either reward or salient stimuli and the social-cognitive system, as long timescale regions, are accumulating information regarding the participant's social partner across the entire experiment, then this could account for our lack of context-dependent differences in connectivity between these two regions.

To test this hypothesis, future work is needed in multiple areas. First, rather than assuming that each region functions on the same timescale, researchers should examine brain network dynamics as a series of nested systems that respond to in-

formation over multiple timescales, possibly using methods such as inter-subject functional connectivity (Simony et al., 2016). Second, greater care should be taken to accurately assess the complex dynamics within- and between-system organization in general (Ashourvan et al., 2017; Calhoun et al., 2014). And third, such dynamics need to be better characterized during cognitive tasks (Cole et al., 2019; Venkatesh et al., 2019). One limitation of the current study is that our event timing was such that events were too short to accurately estimate such dynamics.

## 4.6 Conclusion

In conclusion, the current dissertation was the first study to examine the functional relationship between brain systems implicated in reward and social-cognitive processing in participants who are neurotypical and those with ASD during a real-time social interaction. We use a novel Bayesian statistical analysis, which pools data from multiple ROIs to examine the posterior distributions surrounding the effects-of-interest within our own data, thus removing the issue of multiple comparisons and increasing our ability to infer effects. Contrary to our hypotheses, we found evidence that the reward and social-cognitive systems exhibit age-related changes in functional connectivity such that they become integrated during the absence of a social reward and during the receipt of a non-social reward, casting doubt on the predominant theory of how these systems interact during social reward processing. Further, we did not find evidence that those with ASD exhibit atypical connectivity between reward and social brain systems during a social interaction.

Our results have important implications for understanding how the neurotypical and atypical human brain responds to motivating and rewarding social stimuli and underscores the importance of examining multidimensional heterogeneity within- and between-groups.

# Appendix A: ROI Posterior Distribution Tables

Table A.1: Aim 1 main model ROI results. Posterior distributions are presented in Figure 3.2. Values in ***bold and italics*** denote distributions whose 95% quantile does not overlap with 0 whereas values in *italics* denote distributions whose 90% quantile does not overalp wih 0.

| Contrast | ROI | $\beta_{intercept}$ | SD | 2.5% | 97.5% |
|---|---|---|---|---|---|
| Peer > Computer Initiation | vmPFC | -0.028 | 0.034 | -0.097 | 0.038 |
| | Amygdala | -0.014 | 0.035 | -0.081 | 0.055 |
| | ATL | -0.013 | 0.035 | -0.081 | 0.055 |
| | dmPFC | -0.055 | 0.040 | -0.135 | 0.020 |
| | Left TPJ | -0.026 | 0.035 | -0.096 | 0.042 |
| | Right TPJ | -0.025 | 0.034 | -0.093 | 0.042 |
| | Precuneus | -0.016 | 0.035 | -0.083 | 0.053 |
| | Motor | -0.020 | 0.034 | -0.087 | 0.046 |
| | Auditory | -0.030 | 0.034 | -0.099 | 0.037 |
| | Visual | -0.028 | 0.034 | -0.097 | 0.038 |
| Main effect Partner | vmPFC | -0.169 | 0.144 | -0.465 | 0.098 |
| | Amygdala | -0.002 | 0.117 | -0.232 | 0.231 |
| | ATL | -0.013 | 0.117 | -0.240 | 0.218 |
| | dmPFC | -0.016 | 0.118 | -0.246 | 0.219 |
| | Left TPJ | 0.073 | 0.128 | -0.167 | 0.336 |
| | Right TPJ | -0.023 | 0.115 | -0.248 | 0.203 |
| | Precuneus | -0.024 | 0.117 | -0.256 | 0.204 |
| | Motor | -0.027 | 0.119 | -0.201 | 0.267 |
| | Auditory | -0.022 | 0.116 | -0.249 | 0.202 |
| | Visual | -0.031 | 0.115 | -0.263 | 0.189 |
| Main effect Contingency | vmPFC | -0.018 | 0.098 | -0.205 | 0.179 |
| | Amygdala | -0.021 | 0.099 | -0.211 | 0.178 |
| | ATL | -0.013 | 0.098 | -0.199 | 0.188 |
| | dmPFC | -0.024 | 0.097 | -0.214 | 0.169 |
| | Left TPJ | -0.019 | 0.098 | -0.207 | 0.179 |
| | Right TPJ | -0.022 | 0.097 | -0.210 | 0.172 |
| | Precuneus | -0.034 | 0.098 | -0.227 | 0.158 |
| | Motor | -0.048 | 0.099 | -0.247 | 0.143 |
| | Auditory | -0.033 | 0.097 | -0.226 | 0.156 |
| | Visual | -0.057 | 0.098 | -0.205 | 0.179 |
| Partner $*$ Contingency | vmPFC | 0.089 | 0.094 | -0.093 | 0.280 |
| | Amygdala | 0.064 | 0.094 | -0.126 | 0.245 |
| | ATL | 0.062 | 0.094 | -0.129 | 0.244 |
| | dmPFC | 0.075 | 0.094 | -0.113 | 0.259 |
| | Left TPJ | 0.066 | 0.094 | -0.121 | 0.247 |
| | Right TPJ | 0.059 | 0.095 | -0.134 | 0.240 |
| | Precuneus | 0.083 | 0.094 | -0.100 | 0.270 |
| | Motor | 0.083 | 0.094 | -0.101 | 0.269 |
| | Auditory | 0.072 | 0.094 | -0.117 | 0.256 |
| | Visual | 0.088 | 0.094 | -0.095 | 0.276 |

Table A.2: Aim 1 pairwise reply ROI results. Posterior distributions are presented in Figure 3.4. Values in ***bold and italics*** denote distributions whose 95% quantile does not overlap with 0 whereas values in *italics* denote distributions whose 90% quantile does not overalp wih 0.

| Contrast | ROI | $\beta_{intercept}$ | SD | 2.5% | 97.5% |
|---|---|---|---|---|---|
| Peer Agree > Peer Away | vmPFC | 0.034 | 0.068 | -0.097 | 0.169 |
| | Amygdala | 0.021 | 0.067 | -0.111 | 0.150 |
| | ATL | 0.025 | 0.066 | -0.107 | 0.155 |
| | dmPFC | 0.025 | 0.067 | -0.107 | 0.159 |
| | Left TPJ | 0.024 | 0.067 | -0.108 | 0.155 |
| | Right TPJ | 0.020 | 0.068 | -0.114 | 0.152 |
| | Precuneus | 0.026 | 0.066 | -0.105 | 0.156 |
| | Motor | 0.021 | 0.066 | -0.110 | 0.151 |
| | Auditory | 0.021 | 0.067 | -0.110 | 0.152 |
| | Visual | 0.020 | 0.067 | -0.111 | 0.150 |
| Peer Agree > Computer Agree | vmPFC | 0.003 | 0.071 | -0.145 | 0.137 |
| | Amygdala | 0.023 | 0.068 | -0.114 | 0.157 |
| | ATL | 0.018 | 0.068 | -0.118 | 0.152 |
| | dmPFC | 0.025 | 0.068 | -0.110 | 0.161 |
| | Left TPJ | 0.041 | 0.069 | -0.091 | 0.180 |
| | Right TPJ | 0.017 | 0.068 | -0.119 | 0.151 |
| | Precuneus | 0.030 | 0.068 | -0.103 | 0.166 |
| | Motor | 0.039 | 0.069 | -0.093 | 0.180 |
| | Auditory | 0.022 | 0.067 | -0.113 | 0.154 |
| | Visual | 0.030 | 0.068 | -0.101 | 0.167 |
| Peer Away > Computer Away | vmPFC | -0.121 | 0.094 | -0.316 | 0.048 |
| | Amygdala | -0.027 | 0.080 | -0.181 | 0.134 |
| | ATL | -0.031 | 0.080 | -0.184 | 0.129 |
| | dmPFC | -0.050 | 0.082 | -0.210 | 0.113 |
| | Left TPJ | 0.008 | 0.089 | -0.157 | 0.189 |
| | Right TPJ | -0.029 | 0.081 | -0.184 | 0.132 |
| | Precuneus | -0.062 | 0.080 | -0.223 | 0.094 |
| | Motor | -0.040 | 0.079 | -0.193 | 0.121 |
| | Auditory | -0.047 | 0.079 | -0.202 | 0.108 |
| | Visual | -0.066 | 0.080 | -0.316 | 0.048 |
| Computer Agree > Computer Away | vmPFC | -0.052 | 0.068 | -0.188 | 0.080 |
| | Amygdala | -0.040 | 0.069 | -0.175 | 0.099 |
| | ATL | -0.031 | 0.070 | -0.165 | 0.115 |
| | dmPFC | -0.047 | 0.069 | -0.184 | 0.090 |
| | Left TPJ | -0.039 | 0.069 | -0.172 | 0.099 |
| | Right TPJ | -0.037 | 0.069 | -0.170 | 0.101 |
| | Precuneus | -0.057 | 0.068 | -0.196 | 0.072 |
| | Motor | -0.066 | 0.070 | -0.213 | 0.065 |
| | Auditory | -0.050 | 0.068 | -0.185 | 0.082 |
| | Visual | -0.073 | 0.072 | -0.223 | 0.060 |

Table A.3: Aim 1 main model age results. Posterior distributions are presented in Figure 3.5. Values in ***bold and italics*** denote distributions whose 95% quantile does not overlap with 0 whereas values in *italics* denote distributions whose 90% quantile does not overalp wih 0.

| Contrast | ROI | $\beta_{age}$ | SD | 2.5% | 97.5% |
|---|---|---|---|---|---|
| Peer > Computer Initiation | vmPFC | 0.015 | 0.023 | -0.031 | 0.060 |
| | Amygdala | 0.001 | 0.024 | -0.047 | 0.046 |
| | ATL | -0.005 | 0.025 | -0.053 | 0.042 |
| | dmPFC | 0.040 | 0.025 | -0.009 | 0.089 |
| | Left TPJ | *0.047* | *0.026* | *-0.003* | *0.098* |
| | Right TPJ | 0.007 | 0.024 | -0.040 | 0.052 |
| | Precuneus | 0.023 | 0.023 | -0.023 | 0.069 |
| | Motor | 0.012 | 0.023 | -0.033 | 0.058 |
| | Auditory | 0.015 | 0.023 | -0.030 | 0.060 |
| | Visual | 0.013 | 0.023 | -0.034 | 0.059 |
| Main effect Partner | vmPFC | 0.122 | 0.079 | -0.029 | 0.282 |
| | Amygdala | 0.061 | 0.074 | -0.090 | 0.202 |
| | ATL | 0.045 | 0.077 | -0.113 | 0.188 |
| | dmPFC | 0.139 | 0.082 | -0.014 | 0.309 |
| | Left TPJ | 0.127 | 0.080 | -0.240 | 0.288 |
| | Right TPJ | 0.094 | 0.073 | -0.052 | 0.240 |
| | Precuneus | 0.074 | 0.074 | -0.075 | 0.214 |
| | Motor | 0.061 | 0.075 | -0.090 | 0.204 |
| | Auditory | 0.050 | 0.075 | -0.105 | 0.193 |
| | Visual | 0.069 | 0.074 | -0.083 | 0.211 |
| Main effect Contingency | vmPFC | 0.091 | 0.062 | -0.011 | 0.217 |
| | Amygdala | 0.074 | 0.063 | -0.052 | 0.196 |
| | ATL | 0.078 | 0.062 | -0.045 | 0.199 |
| | dmPFC | 0.084 | 0.062 | -0.038 | 0.205 |
| | Left TPJ | 0.072 | 0.063 | -0.054 | 0.195 |
| | Right TPJ | 0.080 | 0.061 | -0.042 | 0.202 |
| | Precuneus | 0.078 | 0.062 | -0.045 | 0.200 |
| | Motor | 0.083 | 0.062 | -0.038 | 0.205 |
| | Auditory | 0.091 | 0.062 | -0.029 | 0.219 |
| | Visual | 0.087 | 0.062 | -0.030 | 0.217 |
| Partner $*$ Contingency | vmPFC | -0.102 | 0.063 | -0.224 | 0.022 |
| | Amygdala | *-0.109* | *0.062* | *-0.232* | *0.012* |
| | ATL | *-0.105* | *0.062* | *-0.229* | *0.018* |
| | dmPFC | -0.101 | 0.063 | -0.224 | 0.023 |
| | Left TPJ | ***-0.126*** | ***0.065*** | ***-0.262*** | ***-0.004*** |
| | Right TPJ | ***-0.133*** | ***0.067*** | ***-0.273*** | ***-0.007*** |
| | Precuneus | -0.094 | 0.063 | -0.215 | 0.036 |
| | Motor | -0.097 | 0.063 | -0.220 | 0.028 |
| | Auditory | -0.094 | 0.064 | -0.217 | 0.034 |
| | Visual | -0.100 | 0.062 | -0.222 | 0.022 |

Table A.4: Aim 1 reply pairwise ROI results. Posterior distributions are presented in Figure 3.6. Values in ***bold and italics*** denote distributions whose 95% quantile does not overlap with 0 whereas values in *italics* denote distributions whose 90% quantile does not overalp wih 0.

| Contrast | ROI | $\beta_{age}$ | SD | 2.5% | 97.5% |
|---|---|---|---|---|---|
| Peer Agree > Peer Away | vmPFC | 0.002 | 0.047 | -0.087 | 0.095 |
| | Amygdala | -0.018 | 0.047 | -0.111 | 0.073 |
| | ATL | -0.010 | 0.046 | -0.101 | 0.080 |
| | dmPFC | -0.002 | 0.047 | -0.093 | 0.093 |
| | Left TPJ | -0.029 | 0.049 | -0.129 | 0.064 |
| | Right TPJ | -0.028 | 0.049 | -0.129 | 0.065 |
| | Precuneus | -0.005 | 0.046 | -0.095 | 0.086 |
| | Motor | -0.003 | 0.046 | -0.093 | 0.091 |
| | Auditory | 0.007 | 0.048 | -0.085 | 0.106 |
| | Visual | -0.001 | 0.046 | -0.087 | 0.095 |
| Peer Agree > Computer Agree | vmPFC | 0.001 | 0.045 | -0.086 | 0.094 |
| | Amygdala | -0.017 | 0.045 | -0.107 | 0.069 |
| | ATL | -0.019 | 0.045 | -0.108 | 0.069 |
| | dmPFC | 0.008 | 0.047 | -0.080 | 0.107 |
| | Left TPJ | -0.008 | 0.044 | -0.094 | 0.079 |
| | Right TPJ | -0.020 | 0.045 | -0.111 | 0.067 |
| | Precuneus | -0.008 | 0.044 | -0.094 | 0.080 |
| | Motor | -0.011 | 0.044 | -0.097 | 0.075 |
| | Auditory | -0.011 | 0.044 | -0.098 | 0.074 |
| | Visual | -0.011 | 0.044 | -0.098 | 0.076 |
| Peer Away > Computer Away | vmPFC | ***0.103*** | ***0.053*** | ***0.002*** | ***0.210*** |
| | Amygdala | 0.084 | 0.052 | -0.017 | 0.185 |
| | ATL | 0.073 | 0.053 | -0.035 | 0.173 |
| | dmPFC | ***0.112*** | ***0.055*** | ***0.009*** | ***0.223*** |
| | Left TPJ | ***0.132*** | ***0.058*** | ***0.026*** | ***0.252*** |
| | Right TPJ | ***0.119*** | ***0.054*** | ***0.017*** | ***0.230*** |
| | Precuneus | 0.072 | 0.053 | -0.035 | 0.172 |
| | Motor | 0.075 | 0.052 | -0.031 | 0.175 |
| | Auditory | 0.066 | 0.054 | -0.044 | 0.168 |
| | Visual | 0.080 | 0.052 | -0.025 | 0.180 |
| Computer Agree > Computer Away | vmPFC | ***0.093*** | ***0.043*** | ***0.011*** | ***0.179*** |
| | Amygdala | ***0.088*** | ***0.043*** | ***0.004*** | ***0.172*** |
| | ATL | ***0.088*** | ***0.043*** | ***0.004*** | ***0.172*** |
| | dmPFC | ***0.089*** | ***0.043*** | ***0.004*** | ***0.174*** |
| | Left TPJ | ***0.092*** | ***0.043*** | ***0.009*** | ***0.177*** |
| | Right TPJ | ***0.098*** | ***0.043*** | ***0.014*** | ***0.185*** |
| | Precuneus | *0.084* | *0.043* | *-0.002* | *0.167* |
| | Motor | ***0.088*** | ***0.043*** | ***0.004*** | ***0.172*** |
| | Auditory | ***0.090*** | ***0.043*** | ***0.007*** | ***0.175*** |
| | Visual | ***0.091*** | ***0.043*** | ***0.007*** | ***0.175*** |

Table A.5: Aim 2 main model group ROI results. Posterior distributions are presented in Figure 3.8. Values in ***bold and italics*** denote distributions whose 95% quantile does not overlap with 0 whereas values in *italics* denote distributions whose 90% quantile does not overalp wih 0.

| Contrast | ROI | $\beta_{group}$ | SD | 2.5% | 97.5% |
|---|---|---|---|---|---|
| Peer > Computer Initiation | vmPFC | -0.020 | 0.062 | -0.140 | 0.105 |
| | Amygdala | -0.036 | 0.061 | -0.157 | 0.084 |
| | ATL | -0.028 | 0.062 | -0.148 | 0.094 |
| | dmPFC | -0.035 | 0.063 | -0.160 | 0.091 |
| | Left TPJ | -0.012 | 0.065 | -0.134 | 0.120 |
| | Right TPJ | -0.038 | 0.062 | -0.160 | 0.085 |
| | Precuneus | -0.042 | 0.062 | -0.164 | 0.080 |
| | Motor | -0.026 | 0.061 | -0.144 | 0.096 |
| | Auditory | -0.047 | 0.063 | -0.173 | 0.077 |
| | Visual | -0.039 | 0.063 | -0.164 | 0.084 |
| Main effect Partner | vmPFC | -0.163 | 0.187 | -0.536 | 0.205 |
| | Amygdala | -0.109 | 0.185 | -0.462 | 0.269 |
| | ATL | -0.149 | 0.185 | -0.516 | 0.216 |
| | dmPFC | -0.161 | 0.187 | -0.535 | 0.202 |
| | Left TPJ | -0.101 | 0.190 | -0.459 | 0.291 |
| | Right TPJ | -0.157 | 0.183 | -0.518 | 0.202 |
| | Precuneus | -0.162 | 0.184 | -0.528 | 0.199 |
| | Motor | -0.117 | 0.185 | -0.469 | 0.255 |
| | Auditory | -0.154 | 0.183 | -0.510 | 0.210 |
| | Visual | -0.166 | 0.184 | -0.530 | 0.195 |
| Main effect Contingency | vmPFC | 0.044 | 0.179 | -0.298 | 0.408 |
| | Amygdala | 0.012 | 0.175 | -0.328 | 0.355 |
| | ATL | 0.005 | 0.174 | -0.337 | 0.349 |
| | dmPFC | 0.015 | 0.175 | -0.328 | 0.359 |
| | Left TPJ | 0.019 | 0.175 | -0.322 | 0.364 |
| | Right TPJ | -0.003 | 0.175 | -0.350 | 0.339 |
| | Precuneus | -0.026 | 0.179 | -0.386 | 0.319 |
| | Motor | -0.006 | 0.175 | -0.352 | 0.336 |
| | Auditory | -0.006 | 0.175 | -0.359 | 0.335 |
| | Visual | 0.019 | 0.178 | -0.330 | 0.373 |
| Partner $*$ Contingency | vmPFC | -0.287 | 0.205 | -0.685 | 0.123 |
| | Amygdala | -0.285 | 0.207 | -0.686 | 0.217 |
| | ATL | -0.311 | 0.204 | -0.710 | 0.094 |
| | dmPFC | -0.338 | 0.211 | -0.755 | 0.072 |
| | Left TPJ | -0.326 | 0.207 | -0.742 | 0.078 |
| | Right TPJ | -0.339 | 0.210 | -0.762 | 0.069 |
| | Precuneus | -0.290 | 0.207 | -0.693 | 0.125 |
| | Motor | -0.259 | 0.207 | -0.651 | 0.163 |
| | Auditory | -0.251 | 0.209 | -0.642 | 0.175 |
| | Visual | -0.244 | 0.211 | -0.639 | 0.187 |

Table A.6: Aim 2 reply pairwise group ROI results. Posterior distributions are presented in Figure 3.10. Values in ***bold and italics*** denote distributions whose 95% quantile does not overlap with 0 whereas values in *italics* denote distributions whose 90% quantile does not overalp wih 0.

| Contrast | ROI | $\beta_{group}$ | SD | 2.5% | 97.5% |
|---|---|---|---|---|---|
| Peer Agree > Peer Away | vmPFC | -0.124 | 0.136 | -0.389 | 0.146 |
| | Amygdala | -0.140 | 0.133 | -0.418 | 0.124 |
| | ATL | -0.152 | 0.133 | -0.418 | 0.107 |
| | dmPFC | -0.158 | 0.135 | -0.429 | 0.103 |
| | Left TPJ | -0.154 | 0.134 | -0.425 | 0.106 |
| | Right TPJ | -0.166 | 0.136 | -0.440 | 0.094 |
| | Precuneus | -0.161 | 0.136 | -0.435 | 0.100 |
| | Motor | -0.137 | 0.133 | -0.400 | 0.125 |
| | Auditory | -0.133 | 0.134 | -0.398 | 0.132 |
| | Visual | -0.117 | 0.137 | -0.381 | 0.160 |
| Peer Agree > Computer Agree | vmPFC | *-0.221* | *0.128* | *-0.473* | *0.035* |
| | Amygdala | -0.195 | 0.131 | -0.445 | 0.072 |
| | ATL | *-0.229* | *0.127* | *-0.481* | *0.022* |
| | dmPFC | *-0.252* | *0.134* | *-0.523* | *0.003* |
| | Left TPJ | *-0.213* | *0.128* | *-0.461* | *0.044* |
| | Right TPJ | *-0.244* | *0.130* | *-0.507* | *0.007* |
| | Precuneus | *-0.230* | *0.128* | *-0.483* | *0.019* |
| | Motor | -0.191 | 0.131 | -0.441 | 0.077 |
| | Auditory | -0.204 | 0.129 | -0.449 | 0.062 |
| | Visual | -0.213 | 0.129 | -0.473 | 0.046 |
| Peer Away > Computer Away | vmPFC | 0.049 | 0.151 | -0.257 | 0.338 |
| | Amygdala | 0.090 | 0.149 | -0.204 | 0.384 |
| | ATL | 0.074 | 0.148 | -0.218 | 0.365 |
| | dmPFC | 0.092 | 0.150 | -0.202 | 0.388 |
| | Left TPJ | 0.119 | 0.155 | -0.179 | 0.436 |
| | Right TPJ | 0.090 | 0.148 | -0.201 | 0.382 |
| | Precuneus | 0.058 | 0.148 | -0.241 | 0.344 |
| | Motor | 0.070 | 0.147 | -0.225 | 0.361 |
| | Auditory | 0.048 | 0.149 | -0.253 | 0.331 |
| | Visual | 0.036 | 0.152 | -0.275 | 0.323 |
| Computer Agree > Computer Away | vmPFC | 0.162 | 0.134 | -0.099 | 0.432 |
| | Amygdala | 0.148 | 0.134 | -0.120 | 0.411 |
| | ATL | 0.158 | 0.134 | -0.102 | 0.422 |
| | dmPFC | 0.169 | 0.136 | -0.093 | 0.442 |
| | Left TPJ | 0.166 | 0.136 | -0.096 | 0.439 |
| | Right TPJ | 0.163 | 0.136 | -0.099 | 0.433 |
| | Precuneus | 0.134 | 0.136 | -0.138 | 0.395 |
| | Motor | 0.130 | 0.135 | -0.141 | 0.389 |
| | Auditory | 0.127 | 0.136 | -0.149 | 0.387 |
| | Visual | 0.139 | 0.135 | -0.129 | 0.406 |

Table A.7: Aim 2 reply main model ASD age results. Posterior distributions are presented in Figure 3.11. Values in ***bold and italics*** denote distributions whose 95% quantile does not overlap with 0 whereas values in *italics* denote distributions whose 90% quantile does not overalp wih 0.

| Contrast | ROI | $\beta_{age}$ | SD | 2.5% | 97.5% |
|---|---|---|---|---|---|
| Peer > Computer Initiation | vmPFC | -0.001 | 0.022 | -0.045 | 0.043 |
| | Amygdala | 0.001 | 0.022 | -0.043 | 0.046 |
| | ATL | 0.001 | 0.023 | -0.043 | 0.047 |
| | dmPFC | 0.002 | 0.023 | -0.041 | 0.048 |
| | Left TPJ | -0.004 | 0.022 | -0.049 | 0.004 |
| | Right TPJ | -0.005 | 0.022 | -0.050 | 0.039 |
| | Precuneus | -0.005 | 0.023 | -0.051 | 0.039 |
| | Motor | 0.003 | 0.022 | -0.047 | 0.041 |
| | Auditory | -0.003 | 0.022 | -0.047 | 0.042 |
| | Visual | 0.000 | 0.023 | -0.044 | 0.045 |
| Main effect Partner | vmPFC | 0.053 | 0.075 | -0.108 | 0.187 |
| | Amygdala | 0.101 | 0.066 | -0.030 | 0.234 |
| | ATL | 0.078 | 0.068 | -0.061 | 0.206 |
| | dmPFC | ***0.138*** | ***0.072*** | ***0.004*** | ***0.291*** |
| | Left TPJ | *0.115* | *0.067* | *-0.014* | *0.251* |
| | Right TPJ | 0.102 | 0.066 | -0.027 | 0.231 |
| | Precuneus | 0.085 | 0.068 | -0.055 | 0.215 |
| | Motor | *0.121* | *0.068* | *-0.008* | *0.261* |
| | Auditory | *0.111* | *0.066* | *-0.017* | *0.246* |
| | Visual | *0.111* | *0.075* | *-0.108* | *0.187* |
| Main effect Contingency | vmPFC | -0.035 | 0.073 | -0.187 | 0.102 |
| | Amygdala | 0.008 | 0.068 | -0.146 | 0.125 |
| | ATL | 0.003 | 0.068 | -0.132 | 0.138 |
| | dmPFC | 0.006 | 0.070 | -0.132 | 0.146 |
| | Left TPJ | -0.027 | 0.071 | -0.172 | 0.107 |
| | Right TPJ | 0.008 | 0.068 | -0.125 | 0.144 |
| | Precuneus | 0.013 | 0.069 | -0.122 | 0.151 |
| | Motor | 0.010 | 0.069 | -0.123 | 0.146 |
| | Auditory | -0.028 | 0.071 | -0.173 | 0.107 |
| | Visual | 0.044 | 0.077 | -0.100 | 0.202 |
| Partner $*$ Contingency | vmPFC | -0.125 | 0.080 | -0.285 | 0.031 |
| | Amygdala | -0.115 | 0.080 | -0.273 | 0.041 |
| | ATL | -0.105 | 0.080 | -0.260 | 0.057 |
| | dmPFC | *-0.160* | *0.090* | *-0.346* | *0.006* |
| | Left TPJ | -0.119 | 0.080 | -0.276 | 0.037 |
| | Right TPJ | -0.105 | 0.080 | -0.262 | 0.055 |
| | Precuneus | -0.105 | 0.081 | -0.261 | 0.059 |
| | Motor | -0.111 | 0.080 | -0.267 | 0.048 |
| | Auditory | -0.088 | 0.083 | -0.245 | 0.084 |
| | Visual | -0.098 | 0.081 | -0.253 | 0.031 |

Table A.8: Aim 2 reply pairwise ASD age ROI results. Posterior distributions are presented in Figure 3.12. Values in ***bold and italics*** denote distributions whose 95% quantile does not overlap with 0 whereas values in *italics* denote distributions whose 90% quantile does not overalp wih 0.

| Contrast | ROI | $\beta_{age}$ | SD | 2.5% | 97.5% |
|---|---|---|---|---|---|
| Peer Agree > Peer Away | vmPFC | -0.085 | 0.057 | -0.202 | 0.022 |
| | Amygdala | -0.069 | 0.054 | -0.175 | 0.036 |
| | ATL | -0.058 | 0.054 | -0.162 | 0.051 |
| | dmPFC | -0.088 | 0.058 | -0.208 | 0.021 |
| | Left TPJ | -0.078 | 0.055 | -0.188 | 0.029 |
| | Right TPJ | -0.056 | 0.055 | -0.162 | 0.055 |
| | Precuneus | -0.054 | 0.055 | -0.160 | 0.061 |
| | Motor | -0.057 | 0.054 | -0.163 | 0.052 |
| | Auditory | -0.063 | 0.054 | -0.170 | 0.043 |
| | Visual | -0.037 | 0.058 | -0.146 | 0.084 |
| Peer Agree > Computer Agree | vmPFC | -0.029 | 0.052 | -0.140 | 0.068 |
| | Amygdala | -0.006 | 0.048 | -0.100 | 0.090 |
| | ATL | -0.011 | 0.048 | -0.107 | 0.084 |
| | dmPFC | -0.016 | 0.049 | -0.114 | 0.078 |
| | Left TPJ | -0.003 | 0.047 | -0.095 | 0.092 |
| | Right TPJ | -0.002 | 0.048 | -0.097 | 0.094 |
| | Precuneus | -0.008 | 0.048 | -0.103 | 0.087 |
| | Motor | 0.004 | 0.049 | -0.091 | 0.103 |
| | Auditory | 0.010 | 0.050 | -0.084 | 0.115 |
| | Visual | 0.005 | 0.048 | -0.087 | 0.104 |
| Peer Away > Computer Away | vmPFC | 0.091 | 0.057 | -0.026 | 0.198 |
| | Amygdala | ***0.112*** | ***0.055*** | ***0.004*** | ***0.221*** |
| | ATL | 0.094 | 0.056 | -0.021 | 0.199 |
| | dmPFC | *0.156* | *0.065* | *0.038* | *0.293* |
| | Left TPJ | ***0.122*** | ***0.055*** | ***0.016*** | ***0.233*** |
| | Right TPJ | *0.106* | *0.055* | *-0.003* | *0.214* |
| | Precuneus | *0.097* | *0.056* | *-0.016* | *0.203* |
| | Motor | ***0.117*** | ***0.055*** | ***0.010*** | ***0.226*** |
| | Auditory | *0.101* | *0.055* | *-0.011* | *0.207* |
| | Visual | *0.105* | *0.055* | *-0.003* | *0.198* |
| Computer Agree > Computer Away | vmPFC | 0.049 | 0.050 | -0.051 | 0.144 |
| | Amygdala | 0.054 | 0.049 | -0.044 | 0.149 |
| | ATL | 0.055 | 0.049 | -0.042 | 0.153 |
| | dmPFC | *0.087* | *0.055* | *-0.015* | *0.201* |
| | Left TPJ | 0.049 | 0.050 | -0.050 | 0.146 |
| | Right TPJ | 0.053 | 0.049 | -0.046 | 0.149 |
| | Precuneus | 0.060 | 0.050 | -0.038 | 0.160 |
| | Motor | 0.058 | 0.050 | -0.039 | 0.158 |
| | Auditory | 0.029 | 0.054 | -0.082 | 0.128 |
| | Visual | 0.069 | 0.051 | -0.028 | 0.173 |

Table A.9: Aim 3 main model post test ROI results. Posterior distributions are presented in Figure 3.13. Values in ***bold and italics*** denote distributions whose 95% quantile does not overlap with 0 whereas values in *italics* denote distributions whose 90% quantile does not overalp wih 0.

| Contrast | ROI | $\beta_{post\_test}$ | SD | 2.5% | 97.5% |
|---|---|---|---|---|---|
| Peer > Computer Initiation | vmPFC | 0.027 | 0.020 | -0.011 | 0.066 |
| | Amygdala | 0.022 | 0.019 | -0.016 | 0.060 |
| | ATL | 0.019 | 0.019 | -0.019 | 0.057 |
| | dmPFC | 0.033 | 0.021 | -0.008 | 0.076 |
| | Left TPJ | 0.024 | 0.019 | -0.014 | 0.063 |
| | Right TPJ | 0.008 | 0.020 | -0.033 | 0.047 |
| | Precuneus | 0.012 | 0.020 | -0.027 | 0.051 |
| | Motor | 0.018 | 0.019 | -0.020 | 0.056 |
| | Auditory | 0.013 | 0.020 | -0.027 | 0.050 |
| | Visual | 0.012 | 0.020 | -0.028 | 0.050 |
| Main effect Partner | vmPFC | 0.056 | 0.061 | -0.062 | 0.179 |
| | Amygdala | 0.048 | 0.060 | -0.071 | 0.166 |
| | ATL | 0.056 | 0.061 | -0.062 | 0.177 |
| | dmPFC | 0.046 | 0.061 | -0.074 | 0.167 |
| | Left TPJ | 0.049 | 0.060 | -0.069 | 0.168 |
| | Right TPJ | 0.050 | 0.060 | -0.067 | 0.166 |
| | Precuneus | 0.050 | 0.059 | -0.065 | 0.166 |
| | Motor | 0.036 | 0.061 | -0.086 | 0.153 |
| | Auditory | 0.049 | 0.060 | -0.067 | 0.166 |
| | Visual | 0.032 | 0.062 | -0.094 | 0.149 |
| Main effect Contingency | vmPFC | 0.034 | 0.042 | -0.047 | 0.120 |
| | Amygdala | 0.021 | 0.041 | -0.061 | 0.101 |
| | ATL | 0.028 | 0.041 | -0.051 | 0.111 |
| | dmPFC | 0.022 | 0.041 | -0.060 | 0.102 |
| | Left TPJ | 0.025 | 0.041 | -0.055 | 0.106 |
| | Right TPJ | 0.013 | 0.043 | -0.072 | 0.095 |
| | Precuneus | 0.023 | 0.041 | -0.057 | 0.104 |
| | Motor | 0.018 | 0.042 | -0.066 | 0.098 |
| | Auditory | 0.029 | 0.042 | -0.052 | 0.114 |
| | Visual | 0.020 | 0.042 | -0.065 | 0.102 |
| Partner $*$ Contingency | vmPFC | -0.014 | 0.062 | -0.136 | 0.108 |
| | Amygdala | -0.002 | 0.063 | -0.122 | 0.126 |
| | ATL | -0.023 | 0.062 | -0.145 | 0.098 |
| | dmPFC | 0.017 | 0.068 | -0.109 | 0.158 |
| | Left TPJ | -0.018 | 0.062 | -0.140 | 0.102 |
| | Right TPJ | -0.016 | 0.062 | -0.139 | 0.107 |
| | Precuneus | -0.063 | 0.071 | -0.211 | 0.066 |
| | Motor | -0.008 | 0.063 | -0.131 | 0.117 |
| | Auditory | -0.024 | 0.062 | -0.150 | 0.095 |
| | Visual | -0.021 | 0.062 | -0.146 | 0.101 |

Table A.10: Aim 3 pairwise reply post test ROI results. Posterior distributions are presented in Figure 3.14. Values in ***bold and italics*** denote distributions whose 95% quantile does not overlap with 0 whereas values in *italics* denote distributions whose 90% quantile does not overalp wih 0.

| Contrast | ROI | $\beta_{post\_test}$ | SD | 2.5% | 97.5% |
|---|---|---|---|---|---|
| Peer Agree > Peer Away | vmPFC | -0.048 | 0.056 | -0.158 | 0.062 |
| | Amygdala | -0.053 | 0.056 | -0.162 | 0.055 |
| | ATL | -0.048 | 0.056 | -0.158 | 0.062 |
| | dmPFC | -0.062 | 0.057 | -0.176 | 0.047 |
| | Left TPJ | -0.045 | 0.057 | -0.153 | 0.069 |
| | Right TPJ | -0.067 | 0.058 | -0.184 | 0.044 |
| | Precuneus | -0.049 | 0.056 | -0.160 | 0.062 |
| | Motor | -0.057 | 0.056 | -0.168 | 0.052 |
| | Auditory | -0.045 | 0.056 | -0.153 | 0.068 |
| | Visual | -0.044 | 0.057 | -0.155 | 0.062 |
| Peer Agree > Computer Agree | vmPFC | -0.015 | 0.042 | -0.099 | 0.065 |
| | Amygdala | -0.001 | 0.041 | -0.080 | 0.081 |
| | ATL | -0.007 | 0.040 | -0.086 | 0.074 |
| | dmPFC | 0.004 | 0.043 | -0.077 | 0.070 |
| | Left TPJ | -0.007 | 0.040 | -0.086 | 0.073 |
| | Right TPJ | -0.007 | 0.040 | -0.088 | 0.072 |
| | Precuneus | -0.009 | 0.040 | -0.091 | 0.070 |
| | Motor | -0.010 | 0.040 | -0.091 | 0.070 |
| | Auditory | -0.007 | 0.040 | -0.087 | 0.072 |
| | Visual | -0.004 | 0.040 | -0.083 | 0.077 |
| Peer Away > Computer Away | vmPFC | -0.043 | 0.044 | -0.128 | 0.044 |
| | Amygdala | -0.038 | 0.044 | -0.123 | 0.052 |
| | ATL | -0.048 | 0.044 | -0.134 | 0.039 |
| | dmPFC | -0.030 | 0.046 | -0.118 | 0.064 |
| | Left TPJ | -0.071 | 0.046 | -0.166 | 0.015 |
| | Right TPJ | -0.060 | 0.044 | -0.149 | 0.024 |
| | Precuneus | *-0.074* | *0.047* | *-0.170* | *0.012* |
| | Motor | -0.024 | 0.047 | -0.111 | 0.074 |
| | Auditory | -0.057 | 0.043 | -0.144 | 0.027 |
| | Visual | -0.044 | 0.043 | -0.129 | 0.042 |
| Computer Agree > Computer Away | vmPFC | -0.029 | 0.039 | -0.106 | 0.047 |
| | Amygdala | -0.029 | 0.039 | -0.106 | 0.046 |
| | ATL | -0.021 | 0.039 | -0.095 | 0.057 |
| | dmPFC | -0.027 | 0.039 | -0.104 | 0.049 |
| | Left TPJ | -0.026 | 0.039 | -0.102 | 0.051 |
| | Right TPJ | -0.024 | 0.039 | -0.099 | 0.054 |
| | Precuneus | -0.042 | 0.042 | -0.131 | 0.035 |
| | Motor | -0.021 | 0.039 | -0.095 | 0.058 |
| | Auditory | -0.026 | 0.038 | -0.103 | 0.050 |
| | Visual | -0.010 | 0.041 | -0.087 | 0.078 |

Table A.11: Aim 3 main model SRS ROI results. Posterior distributions are presented in Figure 3.15. Values in ***bold and italics*** denote distributions whose 95% quantile does not overlap with 0 whereas values in *italics* denote distributions whose 90% quantile does not overalp wih 0.

| Contrast | ROI | $\beta_{SRS}$ | SD | 2.5% | 97.5% |
|---|---|---|---|---|---|
| Peer > Computer Initiation | vmPFC | 0.004 | 0.004 | -0.004 | 0.012 |
| | Amygdala | 0.005 | 0.004 | -0.003 | 0.013 |
| | ATL | 0.005 | 0.004 | -0.002 | 0.013 |
| | dmPFC | 0.004 | 0.004 | -0.005 | 0.012 |
| | Left TPJ | 0.004 | 0.004 | -0.004 | 0.012 |
| | Right TPJ | 0.006 | 0.004 | -0.002 | 0.014 |
| | Precuneus | *0.007* | *0.004* | *-0.001* | *0.015* |
| | Motor | 0.005 | 0.004 | -0.003 | 0.013 |
| | Auditory | *0.007* | *0.004* | *-0.001* | *0.015* |
| | Visual | *0.008* | *0.004* | *0.000* | *0.017* |
| Main effect Partner | vmPFC | 0.002 | 0.002 | -0.002 | 0.007 |
| | Amygdala | 0.001 | 0.002 | -0.003 | 0.006 |
| | ATL | 0.002 | 0.002 | -0.003 | 0.006 |
| | dmPFC | 0.002 | 0.002 | -0.003 | 0.006 |
| | Left TPJ | 0.001 | 0.002 | -0.003 | 0.005 |
| | Right TPJ | 0.002 | 0.002 | -0.003 | 0.006 |
| | Precuneus | 0.002 | 0.002 | -0.003 | 0.006 |
| | Motor | 0.001 | 0.002 | -0.004 | 0.005 |
| | Auditory | 0.001 | 0.002 | -0.003 | 0.005 |
| | Visual | 0.002 | 0.002 | -0.002 | 0.006 |
| Main effect Contingency | vmPFC | -0.001 | 0.002 | -0.005 | 0.004 |
| | Amygdala | 0.000 | 0.002 | -0.004 | 0.004 |
| | ATL | 0.000 | 0.002 | -0.004 | 0.004 |
| | dmPFC | 0.000 | 0.002 | -0.005 | 0.004 |
| | Left TPJ | -0.001 | 0.002 | -0.005 | 0.003 |
| | Right TPJ | 0.000 | 0.002 | -0.004 | 0.004 |
| | Precuneus | 0.000 | 0.002 | -0.004 | 0.004 |
| | Motor | 0.000 | 0.002 | -0.004 | 0.005 |
| | Auditory | 0.000 | 0.002 | -0.004 | 0.004 |
| | Visual | 0.000 | 0.002 | -0.005 | 0.004 |
| Partner $*$ Contingency | vmPFC | 0.002 | 0.002 | -0.002 | 0.006 |
| | Amygdala | 0.001 | 0.002 | -0.003 | 0.006 |
| | ATL | 0.023 | 0.002 | -0.003 | 0.006 |
| | dmPFC | 0.017 | 0.002 | -0.002 | 0.007 |
| | Left TPJ | 0.018 | 0.002 | -0.003 | 0.006 |
| | Right TPJ | 0.016 | 0.002 | -0.003 | 0.006 |
| | Precuneus | 0.063 | 0.002 | -0.003 | 0.006 |
| | Motor | 0.008 | 0.002 | -0.003 | 0.006 |
| | Auditory | 0.024 | 0.002 | -0.003 | 0.005 |
| | Visual | 0.021 | 0.002 | -0.004 | 0.005 |

Table A.12: Aim 3 pairwise reply SRS ROI results. Posterior distributions are presented in Figure 3.16. Values in ***bold and italics*** denote distributions whose 95% quantile does not overlap with 0 whereas values in *italics* denote distributions whose 90% quantile does not overalp wih 0.

| Contrast | ROI | $\beta_{SRS}$ | SD | 2.5% | 97.5% |
|---|---|---|---|---|---|
| Peer Agree > Peer Away | vmPFC | 0.000 | 0.002 | -0.003 | 0.003 |
| | Amygdala | 0.000 | 0.002 | -0.003 | 0.003 |
| | ATL | 0.000 | 0.002 | -0.003 | 0.003 |
| | dmPFC | 0.000 | 0.002 | -0.003 | 0.003 |
| | Left TPJ | 0.000 | 0.002 | -0.003 | 0.003 |
| | Right TPJ | 0.000 | 0.002 | -0.002 | 0.004 |
| | Precuneus | 0.001 | 0.002 | -0.002 | 0.004 |
| | Motor | 0.001 | 0.002 | -0.002 | 0.004 |
| | Auditory | 0.000 | 0.002 | -0.003 | 0.003 |
| | Visual | 0.000 | 0.002 | -0.003 | 0.003 |
| Peer Agree > Computer Agree | vmPFC | 0.002 | 0.002 | -0.001 | 0.005 |
| | Amygdala | 0.001 | 0.002 | -0.002 | 0.004 |
| | ATL | 0.002 | 0.001 | -0.001 | 0.005 |
| | dmPFC | 0.002 | 0.002 | -0.001 | 0.005 |
| | Left TPJ | 0.001 | 0.001 | -0.002 | 0.004 |
| | Right TPJ | 0.002 | 0.001 | -0.001 | 0.005 |
| | Precuneus | 0.002 | 0.001 | -0.001 | 0.005 |
| | Motor | 0.001 | 0.002 | -0.002 | 0.004 |
| | Auditory | 0.001 | 0.002 | -0.002 | 0.004 |
| | Visual | 0.001 | 0.001 | -0.002 | 0.004 |
| Peer Away > Computer Away | vmPFC | 0.000 | 0.002 | -0.003 | 0.003 |
| | Amygdala | 0.000 | 0.002 | -0.004 | 0.003 |
| | ATL | 0.000 | 0.002 | -0.003 | 0.003 |
| | dmPFC | -0.001 | 0.002 | -0.004 | 0.002 |
| | Left TPJ | -0.001 | 0.002 | -0.004 | 0.002 |
| | Right TPJ | 0.000 | 0.002 | -0.003 | 0.003 |
| | Precuneus | 0.000 | 0.002 | -0.003 | 0.003 |
| | Motor | -0.001 | 0.002 | -0.004 | 0.002 |
| | Auditory | 0.000 | 0.002 | -0.003 | 0.003 |
| | Visual | 0.000 | 0.002 | -0.003 | 0.003 |
| Computer Agree > Computer Away | vmPFC | -0.001 | 0.001 | -0.004 | 0.002 |
| | Amygdala | -0.001 | 0.001 | -0.004 | 0.002 |
| | ATL | -0.001 | 0.001 | -0.004 | 0.002 |
| | dmPFC | -0.001 | 0.001 | -0.004 | 0.002 |
| | Left TPJ | -0.001 | 0.001 | -0.004 | 0.002 |
| | Right TPJ | -0.001 | 0.001 | -0.004 | 0.002 |
| | Precuneus | -0.001 | 0.001 | -0.004 | 0.002 |
| | Motor | -0.001 | 0.001 | -0.003 | 0.003 |
| | Auditory | -0.001 | 0.001 | -0.003 | 0.002 |
| | Visual | -0.001 | 0.001 | -0.004 | 0.002 |

# Bibliography

American Psychiatric Association. (2013). *Diagnostic and statistical manual of mental disorders : Dsm-5* (5th ed. ed.). Arlington, VA: American Psychiatric Association.

Anderson, D., Maye, M., & Lord, C. (2011). Changes in maladaptive behaviors from midchildhood to young adulthood in autism spectrum disorder. *Am J Intellect Dev Disabil*, *116*(5), 381–397.

Apperly, I., Warren, F., Andrews, B., Grant, J., & Todd, S. (2011). Developmental continuity in theory of mind: speed and accuracy of belief-desire reasoning in children and adults. *Child Dev*, *82*(5), 1691–1703.

Ashourvan, A., Gu, S., Mattar, M., Vettel, J., & Bassett, D. (2017). The energy landscape underpinning module dynamics in the human brain connectome. *Neuroimage*, *157*, 364–380.

Assaf, M., Hyatt, C., Wong, C., Johnson, M., Schultz, R., Hendler, T., & Pearlson, G. (2013). Mentalizing and motivation neural function during social interactions in autism spectrum disorders. *Neuroimage Clin*, *3*, 321–331.

Bal, E., Yerys, B., Sokoloff, J., Celano, M., Kenworthy, L., Giedd, J., & Wallace, G. (2013). Do social attribution skills improve with age in children with high functioning autism spectrum disorders. *Res Autism Spectr Disord*, *7*(1), 9–16.

Bell, P., & Shine, J. (2016). Subcortical contributions to large-scale network communication. *Neurosci Biobehav Rev*, *71*, 313–322.

Bickart, K., Hollenbeck, M., Barrett, L., & Dickerson, B. (2012). Intrinsic amygdala-

cortical functional connectivity predicts social network size in humans. *J Neurosci*, *32*(42), 14729–14741.

Blackhart, G., Nelson, B., Knowles, M., & Baumeister, R. (2009). Rejection elicits emotional reactions but neither causes immediate distress nor lowers self-esteem: a meta-analytic review of 192 studies on social exclusion. *Pers Soc Psychol Rev*, *13*(4), 269–309.

Bölte, S., Poustka, F., & Constantino, J. (2008). Assessing autistic traits: cross-cultural validation of the social responsiveness scale (srs). *Autism Res*, *1*(6), 354–363.

Bossong, M., & Kahn, R. (2016). The salience of reward. *JAMA Psychiatry*, *73*(8), 777–778.

Bottini, S. (2018). Social reward processing in individuals with autism spectrum disorder: A systematic review of the social motivation hypothesis. *Research in Autism Spectrum Disorders*, *45*, 9–26.

Braams, B., Peters, S., Peper, J., Güro?lu, B., & Crone, E. (2014). Gambling for self, friends, and antagonists: differential contributions of affective and social brain regions on adolescent reward processing. *Neuroimage*, *100*, 281–289.

Calhoun, V., Miller, R., Pearlson, G., & Adal?, T. (2014). The chronnectome: time-varying connectivity networks as the next frontier in fmri data discovery. *Neuron*, *84*(2), 262–274.

Carlson, J., Foti, D., Mujica-Parodi, L., Harmon-Jones, E., & Hajcak, G. (2011). Ventral striatal and medial prefrontal bold activation is correlated with reward-related electrocortical activity: a combined erp and fmri study. *Neuroimage*,

*57*(4), 1608–1616.

Carr, A. (2017). *Social and emotional development in middle childhood child psychology and psychiatry* (Vol. 10). Wiley-Blackwell.

Chaudhuri, R., Knoblauch, K., Gariel, M., Kennedy, H., & Wang, X. (2015). A large-scale circuit mechanism for hierarchical dynamical processing in the primate cortex. *Neuron*, *88*(2), 419–431.

Chavez, R., & Heatherton, T. (2015). Representational similarity of social and valence information in the medial pfc. *J Cogn Neurosci*, *27*(1), 73–82.

Chen, G., Saad, Z., Nath, A., Beauchamp, M., & Cox, R. (2012). Fmri group analysis combining effect estimates and their variances. *Neuroimage*, *60*(1), 747–765.

Chen, G., Xiao, Y., Taylor, P., Rajendra, J., Riggins, T., Geng, F., ... Cox, R. (2019). Handling multiplicity in neuroimaging through bayesian lenses with multilevel modeling. *Neuroinformatics*.

Chen, J., Honey, C., Simony, E., Arcaro, M., Norman, K., & Hasson, U. (2016). Accessing real-life episodic information from minutes versus hours earlier modulates hippocampal and high-order cortical dynamics. *Cereb Cortex*, *26*(8), 3428–3441.

Chevallier, C., Kohls, G., Troiani, V., Brodkin, E., & Schultz, R. (2012). The social motivation theory of autism. *Trends Cogn Sci*, *16*(4), 231–239.

Cisler, J., Bush, K., & Steele, J. (2014). A comparison of statistical methods for detecting context-modulated functional connectivity in fmri. *Neuroimage*, *84*, 1042–1052.

Clements, C., Zoltowski, A., Yankowitz, L., Yerys, B., Schultz, R., & Herrington, J. (2018). Evaluation of the social motivation hypothesis of autism: A systematic review and meta-analysis. *JAMA Psychiatry*.

Clithero, J., & Rangel, A. (2014). Informatic parcellation of the network involved in the computation of subjective value. *Soc Cogn Affect Neurosci*, *9*, 1289–1302.

Cole, M. W., Ito, T., Schultz, D., Mill, R., Chen, R., & Cocuzza, C. (2019). Task activations produce spurious but systematic inflation of task functional connectivity estimates. *NeuroImage*, *189*, 1–18.

Constantino, J. N., & Todd, R. D. (2003). Autistic traits in the general population: a twin study. *Archives of general psychiatry*, *60*(5), 524–530.

Cooper, J., & Knutson, B. (2008). Valence and salience contribute to nucleus accumbens activation. *Neuroimage*, *39*(1), 538–547.

Cox, R. (1996). Afni: software for analysis and visualization of functional magnetic resonance neuroimages. *Comput Biomed Res*, *29*(3), 162–173.

de Bie, H., Boersma, M., Adriaanse, S., Veltman, D., Wink, A., Roosendaal, S., ... Sanz-Arigita, E. (2012). Resting-state networks in awake five- to eight-year old children. *Hum Brain Mapp*, *33*(5), 1189–1201.

Deco, G., Cruzat, J., & Kringelbach, M. (2019). Brain songs framework used for discovering the relevant timescale of the human brain. *Nat Commun*, *10*(1), 583.

Déli, E., Tozzi, A., & Peters, J. (2017). Relationships between short and fast brain timescales. *Cogn Neurodyn*, *11*(6), 539–552.

Di Martino, A., Scheres, A., Margulies, D., Kelly, A., Uddin, L., Shehzad, Z., ...

Milham, M. (2008). Functional connectivity of human striatum: a resting state fmri study. *Cereb Cortex*, *18*(12), 2735–2747.

Dumontheil, I., Apperly, I., & Blakemore, S. (2010). Online usage of theory of mind continues to develop in late adolescence. *Dev Sci*, *13*(2), 331–338.

Easson, A., & McIntosh, A. (2019). Bold signal variability and complexity in children and adolescents with and without autism spectrum disorder. *Dev Cogn Neurosci*, *36*, 100630.

Egger, H., Pine, D., Nelson, E., Leibenluft, E., Ernst, M., Towbin, K., & Angold, A. (2011). The nimh child emotional faces picture set (nimh-chefs): a new set of children's facial emotion stimuli. *Int J Methods Psychiatr Res*, *20*(3), 145–156.

Elton, A., Di Martino, A., Hazlett, H., & Gao, W. (2016). Neural connectivity evidence for a categorical-dimensional hybrid model of autism spectrum disorder. *Biol Psychiatry*, *80*(2), 120–128.

Guyer, A. E., McClure-Tone, E. B., Shiffrin, N. D., Pine, D. S., & Nelson, E. E. (2009). Probing the neural correlates of anticipated peer evaluation in adolescence. *Child development*, *80*(4), 1000–1015.

Gweon, H., Dodell-Feder, D., Bedny, M., & Saxe, R. (2012). Theory of mind performance in children correlates with functional specialization of a brain region for thinking about thoughts. *Child Dev*, *83*(6), 1853–1868.

Haber, S., & Knutson, B. (2010). The reward circuit: linking primate anatomy and human imaging. *Neuropsychopharmacology*, *35*(1), 4–26.

Hare, T., Camerer, C., Knoepfle, D., & Rangel, A. (2010). Value computations in

ventral medial prefrontal cortex during charitable decision making incorporate input from regions involved in social cognition. *J Neurosci*, *30*(2), 583–590.

Hasson, U., Chen, J., & Honey, C. (2015). Hierarchical process memory: memory as an integral component of information processing. *Trends Cogn Sci*, *19*(6), 304–313.

Hasson, U., & Honey, C. (2012). Future trends in neuroimaging: Neural processes as expressed within real-life contexts. *Neuroimage*, *62*(2), 1272–1278.

Hasson, U., Malach, R., & Heeger, D. (2010). Reliability of cortical activity during natural stimulation. *Trends Cogn Sci*, *14*(1), 40–48.

Hasson, U., Yang, E., Vallines, I., Heeger, D., & Rubin, N. (2008). A hierarchy of temporal receptive windows in human cortex. *J Neurosci*, *28*(10), 2539–2550.

Himberger, K., Chien, H., & Honey, C. (2018). Principles of temporal processing across the cortical hierarchy. *Neuroscience*, *389*, 161–174.

Honey, C., Thesen, T., Donner, T., Silbert, L., Carlson, C., Devinsky, O., ... Hasson, U. (2012). Slow cortical dynamics and the accumulation of information over long timescales. *Neuron*, *76*(2), 423–434.

Janowski, V., Camerer, C., & Rangel, A. (2013). Empathic choice involves vmpfc value signals that are modulated by social processing implemented in ipl. *Soc Cogn Affect Neurosci*, *8*(2), 201–208.

Jaswal, V., & Akhtar, N. (2018). Being vs. appearing social uninterested: Challenging assumptions about social motivation in autism. *Behavioral and Brain Sciences*, 1–84.

Jensen, J., Smith, A., Willeit, M., Crawley, A., Mikulis, D., Vitcu, I., & Kapur,

S. (2007). Separate brain regions code for salience vs. valence during reward prediction in humans. *Hum Brain Mapp*, *28*(4), 294–302.

Kahnt, T., Heinzle, J., Park, S., & Haynes, J. (2010). The neural code of reward anticipation in human orbitofrontal cortex. *Proc Natl Acad Sci U S A*, *107*(13), 6010–6015.

Kaufman, A., & Kaufman, N. (2004). *Kaufman brief intelligence scale* (2nd ed.). Bloomington, MN: Pearson, Inc.

Kiebel, S., Daunizeau, J., & Friston, K. (2008). A hierarchy of time-scales and the brain. *PLoS Comput Biol*, *4*(11), e1000209.

Kleiner, M., Brainard, D., & D, P. (2007). What's new in psychtoolbox-3? *Perception*, *36*.

Kohls, G., Perino, M., Taylor, J., Madva, E., Cayless, S., Troiani, V., ... Schultz, R. (2013). The nucleus accumbens is involved in both the pursuit of social reward and the avoidance of social punishment. *Neuropsychologia*, *51*(11), 2062–2069.

Koster-Hale, J., & Saxe, R. (2013). Theory of mind: a neural prediction problem. *Neuron*, *79*(5), 836–848.

Kross, E., Berman, M., Mischel, W., Smith, E., & Wager, T. (2011). Social rejection shares somatosensory representations with physical pain. *Proc Natl Acad Sci U S A*, *108*(15), 6270–6275.

Levy, D., & Glimcher, P. (2012). The root of all value: a neural common currency for choice. *Curr Opin Neurobiol*, *22*(6), 1027–1038.

Liu, J., Lee, H. J., Weitz, A. J., Fang, Z., Lin, P., Choy, M., ... Mitra, P. (2015).

Frequency-selective control of cortical and subcortical networks by central thalamus. *Elife*, *4*, e09215.

Liu, Y., Gao, J.-H., Liotti, M., Pu, Y., & Fox, P. T. (1999). Temporal dissociation of parallel processing in the human subcortical outputs. *Nature*, *400*(6742), 364.

Lord, C., Rutter, M., Goode, S., Heemsbergen, J., Jordan, H., Mawhood, L., & Schopler, E. (1989). Austism diagnostic observation schedule: A standardized observation of communicative and social behavior. *Journal of autism and developmental disorders*, *19*(2), 185–212.

Mazurek, M. O. (2013). Social media use among adults with autism spectrum disorders. *Comput. Hum. Behav.*, *29*(4), 1709–1714.

McLaren, D., Ries, M., Xu, G., & Johnson, S. (2012). A generalized form of context-dependent psychophysiological interactions (gppi): a comparison to standard approaches. *Neuroimage*, *61*(4), 1277–1286.

Monahan, K. C., & Steinberg, L. (2011). Accentuation of individual differences in social competence during the transition to adolescence. *Journal of Research on Adolescence*, *21*(3), 576–585.

Morishima, Y., Schunk, D., Bruhin, A., Ruff, C., & Fehr, E. (2012). Linking brain structure and activation in temporoparietal junction to explain the neurobiology of human altruism. *Neuron*, *75*(1), 73–79.

Moriuchi, J., Klin, A., & Jones, W. (2017). Mechanisms of diminished attention to eyes in autism. *Am J Psychiatry*, *174*(1), 26–35.

Muetzel, R., Blanken, L., Thijssen, S., van der Lugt, A., Jaddoe, V., Verhulst, F.,

... White, T. (2016). Resting-state networks in 6-to-10 year old children. *Hum Brain Mapp*, *37*(12), 4286–4300.

Murray, J., Bernacchia, A., Freedman, D., Romo, R., Wallis, J., Cai, X., ... Wang, X. (2014). A hierarchy of intrinsic timescales across primate cortex. *Nat Neurosci*, *17*(12), 1661–1663.

Nicolle, A., Klein-Flügge, M., Hunt, L., Vlaev, I., Dolan, R., & Behrens, T. (2012). An agent independent axis for executed and modeled choice in medial prefrontal cortex. *Neuron*, *75*(6), 1114–1121.

Parker, J. G., Rubin, K. H., Erath, S. A., Wojslawowicz, J. C., & Buskirk, A. A. (2015). *Peer relationships, child development, and adjustment: A developmental psychopathology perspective developmental psychopathology* (Vol. 12). Wiley-Blackwell.

Pauli, W., O'Reilly, R., Yarkoni, T., & Wager, T. (2016). Regional specialization within the human striatum for diverse psychological functions. *Proc Natl Acad Sci U S A*, *113*(7), 1907–1912.

Peirce, J. (2007). Psychopy–psychophysics software in python. *J Neurosci Methods*, *162*(1-2), 8–13.

Penny, B., & P, S. (2009). The internet: a comfortable communication medium for people with asperger syndrome (as) and high functioning autism (hfa)? *Journal of Assistive Technologies*, *3*(2), 44–53.

Pickering, M., & Garrod, S. (2013). An integrated theory of language production and comprehension. *Behav Brain Sci*, *36*(4), 329–347.

Power, J., Barnes, K., Snyder, A., Schlaggar, B., & Petersen, S. (2012). Spurious

but systematic correlations in functional connectivity mri networks arise from subject motion. *Neuroimage*, *59*(3), 2142–2154.

Power, J., Mitra, A., Laumann, T., Snyder, A., Schlaggar, B., & Petersen, S. (2014). Methods to detect, characterize, and remove motion artifact in resting state fmri. *Neuroimage*, *84*, 320–341.

Redcay, E., Dodell-Feder, D., Mavros, P., Kleiner, M., Pearrow, M., Triantafyllou, C., ... Saxe, R. (2013). Atypical brain activation patterns during a face-to-face joint attention game in adults with autism spectrum disorder. *Hum Brain Mapp*, *34*(10), 2511–2523.

Redcay, E., Dodell-Feder, D., Pearrow, M., Mavros, P., Kleiner, M., Gabrieli, J., & Saxe, R. (2010). Live face-to-face interaction during fmri: a new tool for social cognitive neuroscience. *Neuroimage*, *50*(4), 1639–1647.

Redcay, E., & Warnell, K. R. (2018). A social-interactive neuroscience approach to understanding the developing brain. *Advances in child development and behavior*, *54*, 1–44.

Rice, K., Anderson, L., Velnoskey, K., Thompson, J., & Redcay, E. (2016). Biological motion perception links diverse facets of theory of mind during middle childhood. *J Exp Child Psychol*, *146*, 238–246.

Rice, K., Moriuchi, J., Jones, W., & Klin, A. (2012). Parsing heterogeneity in autism spectrum disorders: visual scanning of dynamic social scenes in school-aged children. *J Am Acad Child Adolesc Psychiatry*, *51*(3), 238–248.

Rice, K., & Redcay, E. (2016). Interaction matters: A perceived social partner alters the neural processing of human speech. *Neuroimage*, *129*, 480–488.

Risko, E., Laidlaw, K., Freeth, M., Foulsham, T., & Kingstone, A. (2012). Social attention with real versus reel stimuli: toward an empirical approach to concerns about ecological validity. *Front Hum Neurosci*, *6*, 143.

Ruff, C., & Fehr, E. (2014). The neurobiology of rewards and values in social decision making. *Nat Rev Neurosci*, *15*(8), 549–562.

Ruge, H., Goschke, T., & Braver, T. (2009). Separating event-related bold components within trials: the partial-trial design revisited. *Neuroimage*, *47*(2), 501–513.

Saxe, R., & Wexler, A. (2005). Making sense of another mind: the role of the right temporo-parietal junction. *Neuropsychologia*, *43*(10), 1391–1399.

Saxe, R., Whitfield-Gabrieli, S., Scholz, J., & Pelphrey, K. A. (2009). Brain regions for perceiving and reasoning about other people in school-aged children. *Child Dev*, *80*(4), 1197–1209.

Schilbach, L., Timmermans, B., Reddy, V., Costall, A., Bente, G., Schlicht, T., & Vogeley, K. (2013). Toward a second-person neuroscience. *Behav Brain Sci*, *36*(4), 393–414.

Schilbach, L., Wilms, M., Eickhoff, S., Romanzetti, S., Tepest, R., Bente, G., ... Vogeley, K. (2010). Minds made for sharing: initiating joint attention recruits reward-related neurocircuitry. *J Cogn Neurosci*, *22*(12), 2702–2715.

Schirmer, A., Meck, W., & Penney, T. (2016). The socio-temporal brain: Connecting people in time. *Trends Cogn Sci*, *20*(10), 760–772.

Schmidt, S., Fenske, S., Kirsch, P., & Mier, D. (2018). Nucleus accumbens activation is linked to salience in social decision making. *Eur Arch Psychiatry Clin*

*Neurosci*.

Schreuders, E., Braams, B., Blankenstein, N., Peper, J., Güro?lu, B., & Crone, E. (2018). Contributions of reward sensitivity to ventral striatum activity across adolescence and early adulthood. *Child Dev*, *89*(3), 797–810.

Schurz, M., Aichhorn, M., Martin, A., & Perner, J. (2013). Common brain areas engaged in false belief reasoning and visual perspective taking: a meta-analysis of functional brain imaging studies. *Front Hum Neurosci*, *7*, 712.

Schurz, M., Radua, J., Aichhorn, M., Richlan, F., & Perner, J. (2014). Fractionating theory of mind: a meta-analysis of functional brain imaging studies. *Neurosci Biobehav Rev*, *42*, 9–34.

Sebanz, N., Bekkering, H., & Knoblich, G. (2006). Joint action: bodies and minds moving together. *Trends Cogn Sci*, *10*(2), 70–76.

Sesack, S., & Grace, A. (2010). Cortico-basal ganglia reward network: microcircuitry. *Neuropsychopharmacology*, *35*(1), 27–47.

Sescousse, G., Li, Y., & Dreher, J. (2015). A common currency for the computation of motivational values in the human striatum. *Soc Cogn Affect Neurosci*, *10*(4), 467–473.

Simony, E., Honey, C., Chen, J., Lositsky, O., Yeshurun, Y., Wiesel, A., & Hasson, U. (2016). Dynamic reconfiguration of the default mode network during narrative comprehension. *Nat Commun*, *7*, 12141.

Smith, D., Clithero, J., Boltuck, S., & Huettel, S. (2014). Functional connectivity with ventromedial prefrontal cortex reflects subjective value for social rewards. *Soc Cogn Affect Neurosci*, *9*(12), 2017–2025.

Supekar, K., Uddin, L., Prater, K., Amin, H., Greicius, M., & Menon, V. (2010). Development of functional and structural connectivity within the default mode network in young children. *Neuroimage*, *52*(1), 290–301.

Tamir, D., & Mitchell, J. (2012). Disclosing information about the self is intrinsically rewarding. *Proc Natl Acad Sci U S A*, *109*(21), 8038–8043.

van den Bos, W., Talwar, A., & McClure, S. (2013). Neural correlates of reinforcement learning and social preferences in competitive bidding. *J Neurosci*, *33*(5), 2137–2146.

van der Meer, M., Kalenscher, T., Lansink, C., Pennartz, C., Berke, J., & Redish, A. (2010). Integrating early results on ventral striatal gamma oscillations in the rat. *Front Neurosci*, *4*, 300.

van der Meer, M., & Redish, A. (2009). Covert expectation-of-reward in rat ventral striatum at decision points. *Front Integr Neurosci*, *3*, 1.

Venkatesh, M., Jaja, J., & Pessoa, L. (2019). Brain dynamics and temporal trajectories during task and naturalistic processing. *Neuroimage*, *186*, 410–423.

Wagner, U., Galli, L., Schott, B., Wold, A., van der Schalk, J., Manstead, A., ... Walter, H. (2015). Beautiful friendship: Social sharing of emotions improves subjective feelings and activates the neural reward circuitry. *Soc Cogn Affect Neurosci*, *10*(6), 801–808.

Wake, S., & Izuma, K. (2017). A common neural code for social and monetary rewards in the human striatum. *Soc Cogn Affect Neurosci*, *12*(10), 1558–1564.

Ward, D., Dill-Shackleford, K., & Mazurek, M. (2018). Social media use and

happiness in adults with autism spectrum disorder. *Cyberpsychol Behav Soc Netw*, *21*(3), 205–209.

Warnell, K., Sadikova, E., & Redcay, E. (2017). Let's chat: developmental neural bases of social motivation during real-time peer interaction. *Dev Sci*.

Watanabe, T., Rees, G., & Masuda, N. (2019). Atypical intrinsic neural timescale in autism. *eLife*, *8*, e42256.

Yarkoni, T., Poldrack, R., Nichols, T., Van Essen, D., & Wager, T. (2011). Large-scale automated synthesis of human functional neuroimaging data. *Nat Methods*, *8*, 665–670.

Zaki, J., & Ochsner, K. (2009). The need for a cognitive neuroscience of naturalistic social cognition. *Ann N Y Acad Sci*, *1167*, 16–30.